

Skew-Probabilistic Neural Networks for Learning from Imbalanced Data

Shraddha M. Naik^a, Tanujit Chakraborty^{1b}, Madhurima Panja^b, Abdenour Hadid^b, Bibhas Chakraborty^{c,d,e}

^a*Khalifa University of Science and Technology, Abu Dhabi, UAE*

^b*Sorbonne University Abu Dhabi, SAFIR, Abu Dhabi, UAE*

^c*Duke-NUS Medical School, National University of Singapore, Singapore*

^d*Department of Statistics and Data Science, National University of Singapore, Singapore*

^e*Department of Biostatistics and Bioinformatics, Duke University, USA*

Abstract

Real-world datasets often exhibit imbalanced data distribution, where certain class levels are severely underrepresented. In such cases, traditional pattern classifiers have shown a bias towards the majority class, impeding accurate predictions for the minority class. This paper introduces an imbalanced data-oriented classifier using probabilistic neural networks (PNN) with a skew-normal kernel function to address this major challenge. PNN is known for providing probabilistic outputs, enabling quantification of prediction confidence, interpretability, and the ability to handle limited data. By leveraging the skew-normal distribution, which offers increased flexibility, particularly for imbalanced and non-symmetric data, our proposed Skew-Probabilistic Neural Networks (SkewPNN) can better represent underlying class densities. Hyperparameter fine-tuning is imperative to optimize the performance of the proposed approach on imbalanced datasets. To this end, we employ a population-based heuristic algorithm, the Bat optimization algorithm, to explore the hyperparameter space effectively. We also prove the statistical consistency of the density estimates, suggesting that the true distribution will be approached smoothly as the sample size increases. Theoretical analysis of the computational complexity of the proposed SkewPNN and BA-SkewPNN is also provided. Numerical simulations have been conducted on different synthetic datasets, comparing various benchmark-imbalanced learners. Real-data analysis on several datasets shows that SkewPNN and BA-SkewPNN substantially outperform most state-of-the-art machine-learning methods for both balanced and imbalanced datasets (binary and multi-class categories) in most experimental settings.

Keywords: Imbalanced classification, Probabilistic neural networks, Skew-normal distribution, Bat algorithm, Consistency.

1. Introduction

Data imbalance is ubiquitous and inherent in real-world applications, encompassing rare event prediction with applications in medical diagnosis, image classification, customer churn prediction, and fraud detection. Instead of preserving an ideal uniform distribution over each class level, real data often exhibit a skewed distribution [49, 52] where specific target value has significantly fewer observations. This situation is known as the “curse of imbalanced data” in the pattern recognition literature [36]. To elaborate more, in applications such as software defect prediction [20], credit card fraud detection [21], medical diagnosis [83], image segmentation [41], etc., events corresponding to different classes are observed with unequal probabilities. For example, classifying between defect-prone and non-defect-prone categories in software modules is of great interest to software engineers, playing a vital role in reducing software development costs and maintaining high quality. The defective class is a minority class, although smaller in number, but it carries more cost

¹Joint First Author and Corresponding Author: tanujit.chakraborty@sorbonne.ae

when misclassified by the software defect prediction models. Similarly, any credit card provider may only observe fewer fraudulent cases among millions of daily transactions. In medical diagnosis, a disease prediction system may find a very limited number of malignant tumor cases compared to many benign cases. All the examples mentioned earlier result in imbalanced data settings where the training set contains an unequal number of instances in the class labels. The imbalanced nature of real-world datasets poses challenges to conventional classifiers, as they tend to favor the majority class (abundance of training instances), resulting in higher misclassification rates for minority class (scarcity of training examples) samples. Therefore, diverse approaches have been introduced to address class imbalance. Existing solutions for learning from imbalanced data can be categorized into data-level and algorithmic-level approaches [52].

Data-level approaches primarily focus on balancing the distribution of samples between the majority and minority classes, ultimately creating a harmonized dataset for learning endeavors [13, 43]. Data-level approaches can be broadly categorized into three primary sub-categories: under-sampling, over-sampling, and mixed-sampling. Several under-sampling techniques have been introduced, including modified versions of random sampling [71, 74], clustering-based approaches [81, 35], and evolutionary algorithm-based approaches [86, 42]. Among these, clustering-based methods (e.g., edited nearest neighbor) share a common approach of grouping samples with similar attributes and selecting a specific number from each cluster based on predefined rules. On the contrary, evolutionary approaches view under-sampling as an optimization challenge within swarm intelligence search algorithms to minimize information loss and mitigate prediction bias. Moving on to oversampling methods, these techniques typically involve duplicating existing minority samples or generating new ones based on specific rules to balance the number of majority and minority instances. A widely recognized approach in this category is the synthetic minority oversampling technique (SMOTE) [24, 37]. SMOTE achieves this by generating new minority instances close to other existing minority examples through interpolation. However, it is worth noting that SMOTE does not consider the data’s density, potentially leading to increased overlap between classes. As a response to this limitation, several extensions of SMOTE have been proposed to address this issue, including majority-weighted minority oversampling [14], borderline-SMOTE [46], adaptive synthetic sampling (ADASYN) [48], convex hull based SMOTE [84], and SMOTE with boosting (SWB) [65]. The mixed-sampling method integrates both under-sampling and over-sampling techniques, effectively mitigating the drawbacks of reduced diversity in the minority class and substantial information loss in the majority class [77, 51]. Alongside the sampling techniques, optimized decision threshold-based frameworks like the Generalized tHreshOld ShiftTing (GHOST) framework have been recently introduced for handling class-imbalance problems [34]. It is worth noting that Generative Adversarial Networks (GANs) also possess a high capability to generate synthetic data and to enhance the performance of data-driven machine learning models, especially with deep learning [22]. However, data-level approaches are very sensitive to the presence of outliers, and sampling strategies excessively distort the data distribution, often resulting in worse performance in real-world scenarios [33].

Algorithm-level techniques encompass the adaptation of established classifiers to enhance their predictive capabilities, particularly with regard to the minority class. Within this domain, an array of strategies has emerged, leveraging well-known classifiers, including support vector machines (SVM) [4], nearest neighbor methods [18, 49], as well as decision trees and random forests [67, 21]. Among the algorithmic-level methods for imbalanced classification, the Hellinger distance decision tree (HDDT), which employs Hellinger distance as the splitting criterion, is a prominent technique in the literature [26]. HDDT, alongside its ensemble counterpart Hellinger distance random forest (HDRF) [28] and other extensions like inter-node HDDT (iHDDT) [3], adeptly handles both balanced and imbalanced datasets. However, HDDTs, while robust against class imbalance, may face overfitting problems due to a lack of pruning [15]. They can also encounter challenges with sticking to local minima and overfitting, particularly with large trees [19]. To avoid these challenges, Hellinger net (HNet) [20] was proposed to tackle the data imbalance challenge for software defect prediction problems. However, the computational expenses resulting from HNet training pose a real challenge when

working with tabular datasets. Also, there is a lack of work on developing neural network-based algorithmic solutions dealing with tabular datasets in the imbalanced domain.

Artificial neural networks (ANNs) have revolutionized machine learning, providing robust solutions for various tasks, including classification and regression [32, 1]. Among the various types of ANNs, probabilistic neural networks (PNN) have gained significant attention due to their distinctive capability of providing probabilistic outputs [69]. This unique feature allows PNN to perform accurate predictions and quantify the uncertainty associated with each prediction, making them highly valuable in dealing with uncertain real-world scenarios. At the heart of PNN lies the utilization of a Gaussian kernel density estimation to model the feature vectors of each class in the training data [58]. This non-parametric kernel-based approach enables the PNN to estimate the probability density function for each class, thereby facilitating accurate classification. However, despite its effectiveness in certain scenarios, the Gaussian kernel may not always be optimal for real-world imbalanced datasets due to their complexities and uncertainties, which a single Gaussian model cannot fully capture. In the classical statistics literature, skew-normal distribution is popular for modeling data with non-zero skewness and asymmetric characteristics [45, 9]. The current work introduces a probabilistic neural network based on the skew-normal kernel function, which we call SkewPNN. Our approach estimates multiple smoothing parameters through a heuristic Bat algorithm. This method is computationally inexpensive and effectively handles benchmark tabular datasets with varied imbalanced settings.

Furthermore, we theoretically show the consistency of the density estimates in SkewPNN so that it can classify data patterns with unknown classes based on the initial set of patterns, the real class of which is known. By shedding light on the benefits of this flexible and adaptable approach, our work lays the foundation for improved decision-making and problem-solving across a wide range of practical applications (balanced and imbalanced data). In essence, our contributions are as follows:

1. We propose two solution strategies, namely SkewPNN and Bat algorithm-based SkewPNN (BA-SkewPNN), utilizing the skew-normal kernel function. Our proposal improves the performance mainly for imbalanced data but also works well for balanced data classification.
2. BA-SkewPNN utilizes a population-based Bat algorithm to optimize the skew-normal kernel function parameters. This strengthens SkewPNN’s ability to handle highly imbalanced data scenarios. A theoretical analysis of the computational complexities of the proposal is also given.
3. We establish theoretical results for the consistency of the density estimates for our proposed method, ensuring that the true distribution will be approached smoothly. Our proposed methods generalize probabilistic neural networks; therefore, they can accurately predict target probability scores.
4. One of the key advantages of our methods is interpretability since it leverages statistical principles to perform classification tasks. The decision boundaries generated by SkewPNN are smoother and more flexible than those generated by the decision tree and random forest-based solution for imbalanced data problems.
5. Experimental results on 20 real imbalanced and 15 real balanced datasets (binary and multiclass) show that the proposed methods are more suitable for imbalanced learning problems than other competitive methods, which is further confirmed by the results of the statistical significance tests.

The rest of the paper is structured as follows. Section 2 provides a comprehensive background on skew-normal distribution, PNN, and the Bat optimization algorithm. In Section 3, the design of the proposed method is presented, along with the introduction of the fitness function used in the Bat algorithm and its theoretical properties. Experimental results and performance analysis are presented in Section 4. Finally, we conclude the paper with a discussion of the findings and future scope for further research in Section 5. Section 6 Appendix gives an illustrative example with numerical values.

2. Preliminaries

This section offers a glimpse into the component methods to be used as building blocks for the proposed methods. We discuss their mathematical formulations and relevance in this study.

2.1. Skew-Normal Distribution

In the last few decades, the skew-normal distribution (both univariate and multivariate) [8, 12, 11, 9] has received great importance for modeling skewed data in statistics, econometrics, nonlinear time series, and finance among many others. The following lemma (for proof, see [9]) played a crucial role in its development:

Lemma 1. *Let $f_0(\cdot)$ be a d -dimensional continuous probability density function (PDF) symmetric around 0. Let G be a one-dimensional cumulative distribution function such that G' (first derivative of G) exists and G' is a density symmetric around 0. Then, $f(x)$ is a density function on \mathbb{R}^d for any (real-valued) odd function $h(x)$ as defined below:*

$$f(x) = 2f_0(x)G\{h(x)\}; \quad x \in \mathbb{R}^d.$$

The above lemma suggests that a symmetric ‘basis’ density f_0 can be manipulated via a perturbation function $G\{h(x)\}$ to get a skewed density $f(x)$. Also, the perturbed density will always include a ‘basis’ density. On using $f_0 = \phi(\cdot)$ (density function of the standard normal distribution) and $G = \Phi(\cdot)$ (distribution function of the standard normal distribution) and $h(x) = \alpha x$, where $\alpha \in \mathbb{R}$, we get the skew-normal distribution with shape parameter α , denoted by $\text{SN}(\alpha)$, and defined as:

$$f(x, \alpha) = 2\phi(x)\Phi(\alpha x); \quad -\infty < x, \alpha < \infty. \quad (1)$$

For $\alpha = 0$, we obtain the standard normal density. A more general form (also called a three-parameter skew-normal distribution) has received considerable attention in the last two decades because of its greater flexibility and applications in various applied fields and is as follows:

$$f(x; \xi, \sigma, \alpha) = \frac{2}{\sigma} \phi\left(\frac{x - \xi}{\sigma}\right) \Phi\left(\frac{\alpha(x - \xi)}{\sigma}\right); \quad -\infty < x, \xi, \alpha < \infty, \sigma > 0,$$

where ξ is the location parameter, σ is the scale parameter and α is a skewness (also known as tilt) parameter. Note that, throughout this manuscript, we represented the scale parameter of both normal and skew-normal distribution by σ to avoid confusion; however, in the experimental setting, the values of σ in normal and skew-normal may be different. Several authors have explored this model to analyze skewed and heavy tail data due to its flexibility [44, 53, 7, 40]. A multivariate extension is straightforward [12] and can be defined as follows: A random vector $\mathbf{X} = (X_1, X_2, \dots, X_d)^T$ is said to follow a d -dimensional multivariate skew-normal distribution if it has the following density function:

$$f_d(\mathbf{x}) = 2\phi_d(\mathbf{x}, \mathbf{\Sigma}) \Phi(\alpha^T \mathbf{x}); \quad \mathbf{x} \in \mathbb{R}^d,$$

where $\phi_d(\mathbf{x}, \mathbf{\Sigma})$ denotes the PDF of d -dimensional multivariate normal with correlation matrix $\mathbf{\Sigma}$ with α is the shape parameter. Inferential statistical properties have been studied, and their successful applications are found to analyze several multivariate datasets in various fields (for e.g., reliability and survival analysis [53]) due to their flexibility.

2.2. Probabilistic Neural Networks (PNN)

Probabilistic neural networks (PNN) are a specialized type of single-pass neural network known for their unique architecture. Unlike multi-pass networks, PNN does not rely on iterative weight adjustments, simplifying their operation and making them well-suited for real-time applications [68]. PNN are particularly notable for their use of Bayesian rules, which enable them to estimate posterior probabilities [68, 63]. As a powerful tool for pattern classification tasks, PNN has garnered significant attention for their capacity

to handle uncertainty and offer valuable insights in various real-world applications. This architecture is characterized by four layers, such as an input layer for processing test patterns, a pattern layer with neurons corresponding to training patterns, a summation layer representing class neurons, and an output layer providing the final classification [68]. PNN has demonstrated their value across various fields, including medicine, science, business, and industries, owing to their ability to handle real-time data effectively [85].

During training, PNN utilizes the Parzen window, a non-parametric density estimation technique, to approximate the underlying data distribution. The working principles of PNN are as follows: (1) Given a new input (test point), the pattern layer computes the similarity between the input and available training samples; (2) The summation layer estimates the probability of the input belonging to each class; and (3) The output layer selects the class with the highest probability. Therefore, for the prediction phase, a winner-takes-all strategy is employed, where the class with the highest probability is selected as the output. This capacity to model the entire PDF empowers PNN to effectively handle both binary and multi-class classification tasks with remarkable accuracy [58]. The training process in PNN is fast as they only need one pass through the training data. In PNN, the Gaussian distribution is favored for its well-understood properties and straightforward mathematical form, characterized by mean (μ) and standard deviation (σ) which defines the shape of the distribution. Within PNN, it is used to estimate class probabilities, associating each training pattern with a Gaussian kernel function centered on its feature values. The spread parameter, determining function width, significantly influences smoothness and generalization. PNN's effective modeling of data distribution using Gaussian kernel makes them suitable for tasks like classification and regression, offering advantages in training, interpretability, and multi-class handling.

Conventional PNN employs the following mathematical formulation to calculate the PDF of a set of random variables X_1, X_2, \dots, X_n with unknown PDF $g(x)$ is estimated using a family of estimators for each class [68] as

$$f_n(x) = \frac{1}{nh(n)} \sum_{i=1}^n K\left(\frac{x - x_i}{h(n)}\right), \quad (2)$$

where $K(\cdot)$ is a kernel function (discussed below) and the bandwidth $h(n)$ constitutes a sequence of numbers satisfying the condition

$$\lim_{n \rightarrow \infty} h(n) = 0. \quad (3)$$

This process entails the utilization of a non-parametric density estimation technique, such as the Parzen window, to approximate the underlying data distribution for each class (c) individually and given as

$$P_c(x) = \frac{f_n(x)}{\sum f_n(x)}. \quad (4)$$

In vector formulation, for a given new input sample x and a training sample x_i from class c , the Gaussian kernel can be represented as

$$K(x, x_i) = \exp\left(-\frac{\|x - x_i\|^2}{2\sigma^2}\right), \quad (5)$$

where σ represents the smoothing parameter (controls the width of the Gaussian kernel), x is the vector representing the input sample, and x_i is the vector representing the training sample from class c . The Gaussian kernel computes the similarity between the new input sample and each training sample, with higher values indicating stronger similarity. It represents a symmetric, bell-shaped curve centered at 0, with the standard deviation determining the width of the curve. Several notable extensions of PNN were introduced in the recent literature, namely weighted PNN [60], self-adaptive PNN [82], and Bat-algorithm-based PNN [61], among many others which addresses the complexities of parameter estimation in PNN. However, none of the above provides a robust solution to the data imbalance problem.

2.3. Bat Algorithm (BA)

Bat algorithm (BA) is a meta-heuristic optimization technique inspired by the echolocation behavior observed in Bats during their foraging activities [79]. It commences by randomly placing a population of B Bats within the search space, with each Bat symbolizing a potential solution to the optimization problem at hand [78, 61].

At every iteration t , the velocity ($v_i(t)$) of each Bat i is updated based on the disparity between its current position ($\varkappa_i(t)$) and the best solution discovered (\varkappa_{best}). The velocity adjustment is regulated by a fixed frequency f_{min} with a maximum limit of f_{max} and dynamic frequency f_i . The velocity $v_i(t+1)$ at time step $t+1$ is determined as

$$v_i(t+1) = v_i(t) + (\varkappa_{\text{best}} - \varkappa_i(t))f_i, \quad (6)$$

where f_i is computed as $f_i = f_{\text{min}} + (f_{\text{max}} - f_{\text{min}})\beta$, with $\beta \in [0, 1]$. Following the velocity update, the new position ($\varkappa_i(t+1)$) of each Bat i is computed by adding the updated velocity to its current position

$$\varkappa_i(t+1) = \varkappa_i(t) + v_i(t+1). \quad (7)$$

Certain Bats may engage in local search by exploring neighboring regions. This is achieved by introducing a random displacement controlled by a parameter ϵ , defined as

$$\varkappa_i(t+1) = \varkappa_i(t) + \epsilon A_t, \quad (8)$$

where A_t represents the average loudness, and $\epsilon \in [-1, 1]$. Initially, the positive loudness A_0 is set. To adapt to evolving conditions during the optimization process, the loudness ($A_i(t+1)$) of each Bat i diminishes over time to decrease the appeal of a solution. This is updated using a scaling factor λ as $A_i(t+1) = \lambda A_i(t)$. Similarly, the pulse rate ($r_i(t+1)$) governs the likelihood of emitting ultrasound pulses and is adjusted throughout the optimization process. BA iterates until a specified stopping condition is fulfilled, which could be reaching a maximum iteration count or attaining a predefined level of precision. This iterative process enables the algorithm to navigate the solution space effectively and ultimately converge toward optimal or highly satisfactory solutions. This versatility and effectiveness render the BA as a valuable and potent tool across a range of problem domains, and this nature-inspired algorithm combined with PNN having a skew-normal kernel is used in this study to address the class imbalance problem.

3. Proposed Method

This section introduces the proposed SkewPNN, followed by Bat algorithm-based SkewPNN and BA-SkewPNN. Furthermore, we study the consistency of density estimates in SkewPNN.

3.1. Algorithm 1: SkewPNN

SkewPNN consists of four layers structured as follows:

- Input Layer: Accept feature vectors of the data.
- Pattern layer: Computes distances between the input vector and each training sample using a similarity measure (skew-normal kernel as defined in Eqn. 10).
- Summation Layer: Aggregates the outputs of the pattern layer for each class.
- Output Layer: Assign the input to the class with the highest posterior probability.

To elaborate, the skew-normal distribution is used as a kernel function in PNN for situations where the data exhibits skewed distributions with a long tail. The skew-normal density, defined by its location parameter ξ , scale parameter σ , and skewness parameter α , is as follows:

$$f(x; \xi, \sigma, \alpha) = \frac{2}{\sigma\sqrt{2\pi}} \exp\left(-\frac{(x-\xi)^2}{2\sigma^2}\right) \Phi\left\{\alpha\left(\frac{x-\xi}{\sigma}\right)\right\}; \quad \xi, x \in (-\infty, \infty), \sigma > 0, \quad (9)$$

where ξ determines the central point of the distribution, σ controls the spread of the distribution, α introduces asymmetry (shape parameter), and $\Phi(z)$ denotes the standard normal cumulative distribution function. For $\alpha = 0$, $f(x)$ is simply the normal distribution where $\alpha > 0$ denotes a longer tail to the right and $\alpha < 0$ denotes the longer tail to the left. The use of skew-normal kernel function will allow the PNN to effectively handle complex and non-symmetric data distributions, making it a valuable choice for various real-world applications. By considering the skewness of the data, the skew-normal kernel enhances the PNN’s ability to provide accurate and probabilistic outputs for classification tasks, particularly when dealing with uncertain and imbalanced datasets. The skew-normal kernel function (without a location parameter) is defined as:

$$K(x, x_i) = \exp\left(-\frac{\|x - x_i\|^2}{2\sigma^2}\right) \Phi\left(\frac{\alpha\|x - x_i\|}{\sigma}\right), \quad (10)$$

where x is the vector representing the new input sample, x_i is the vector representing the training sample from class c , σ represents the smoothing parameter, and Φ denotes the cumulative distribution function (CDF) of the standard normal distribution. The skew-normal kernel function now properly accounts for the smoothing parameter σ in the cumulative distribution term, making it a suitable alternative to the Gaussian kernel (as in Eqn. 5) for handling non-symmetric data distributions in PNN. Incorporating skew-normal kernels introduces asymmetry to the distribution, enabling a more flexible data representation. This plays a pivotal role in PDF computations during both the training and prediction stages of the SkewPNN model, with the selection of the skewness parameter being contingent on the dataset’s characteristics and the specific problem being addressed. In the summation layer of SkewPNN, for a given input x , the class probabilities (for class c) are computed as:

$$P_c(x) = \frac{1}{N_c} \sum_{x_i \in \text{class } c} K(x, x_i),$$

where N_c is the number of training samples in class c . The decision in the output layer is the predicted class \hat{c} , which is the one with the highest posterior probability:

$$\hat{c} = \underset{c}{\operatorname{argmax}} P_c(x).$$

The key difference between standard PNN and SkewPNN lies in the pattern layer activation function, which uses the skew-normal kernel instead of the Gaussian kernel. The hyperparameters in SkewPNN are σ (smoothing parameter) and α (skewness parameter), and adjusting α helps in handling data imbalance problems. Since the Gaussian kernel is a particular case of Eqn. (9) with constant terms, SkewPNN can also be useful for classifying balanced datasets. An illustrative example with numerical values is given in Appendix (Section 6) to explain how the mechanism works in handling imbalanced data.

Remark 1. *The proposed SkewPNN model addresses class imbalance by using the skew-normal kernel, which introduces a skewness parameter (α) to model asymmetrical data distributions adaptively. This parameter enables the kernel to amplify the contribution of minority class samples, ensuring balanced probability estimations across classes. Theoretical properties of the skew-normal distribution ensure that minority class densities are neither underestimated nor dominated by majority class contributions. By naturally reshaping the density estimation process, the SkewPNN framework balances soft probabilistic predictions, improving classification performance in imbalanced settings. In traditional PNN, minority samples contribute mini-*

mally to overall probability scores, whereas SkewPNN’s kernels amplify the influence of minority samples due to their alignment with the underlying skewed distribution.

3.2. Algorithm 2: BA-SkewPNN

For optimizing the parameters of the skew-normal kernel (smoothing parameter σ and skewness parameter α) in SkewPNN, the population-based Bat algorithm is employed. Using the Bat optimization approach, the SkewPNN can fine-tune its parameters effectively and achieve improved performance, especially when dealing with imbalanced datasets and data with asymmetric target distributions. The Bat algorithm’s ability to explore the hyper-parameter space and find suitable solutions enhances the SkewPNN’s capability to handle uncertainty and class imbalance, leading to better classification accuracy and robustness in practical applications. The fitness function in the context of the BA is a crucial component that evaluates the quality of candidate solutions (Bats) during the optimization process. The primary objective of the fitness function is to quantify how well each Bat performs in relation to the optimization problem at hand. It provides a numerical measure of the fitness or suitability of a solution, enabling the algorithm to distinguish between better and worse solutions. In the case of optimizing the parameters of SkewPNN, the fitness function is designed to assess the performance of the SkewPNN on the given classification task. It typically uses performance metrics such as accuracy, F1-score, or area under the receiver operating characteristic curve (AUC-ROC) to measure how well the SkewPNN classifies the data. During each iteration of the Bat Algorithm, the fitness function is applied to evaluate the performance of each Bat’s solution. The algorithm then uses this fitness value to update the Bats’ positions, velocities, loudness, and pulse rates, guiding the search towards better solutions. The goal of the BA is to find the optimal or near-optimal set of hyper-parameters that maximizes the performance of the SkewPNN on the given classification task. By iteratively evaluating and updating the fitness of the candidate solutions, the BA efficiently searches the solution space, eventually converging to a set of hyper-parameters that yields improved classification accuracy and robustness, especially on imbalanced datasets. The fitness function’s design and choice of performance metrics are critical considerations, as they directly influence the success of the optimization process and the final performance of the SkewPNN on the classification task. Given the fitness function, the steps of integrating BA with SkewPNN are as follows:

1. Initialize Population: Randomly initialize B Bats with values for σ and α with predefined ranges

$$\sigma \in [\sigma_{\min}, \sigma_{\max}], \alpha \in [\alpha_{\min}, \alpha_{\max}].$$

2. Update Position and Velocities: Update the positive $\varkappa_i(t)$ and velocity $v_i(t)$ of each Bat at iteration:

$$\begin{aligned} f_i &= f_{\min} + (f_{\max} - f_{\min}) \beta \\ v_i(t+1) &= v_i(t) + (\varkappa_{\text{best}} - \varkappa_i(t)) f_i, \\ \varkappa_i(t+1) &= \varkappa_i(t) + v_i(t+1), \end{aligned}$$

where f_i and β are defined in Section 2.3.

3. Perform Local Search: If a Bat is selected, perform a random walk:

$$\varkappa_{\text{new}} = \varkappa_{\text{current}} + \epsilon A_t,$$

where $\epsilon \in [-1, 1]$ and A_t is loudness at iteration t .

4. Evaluate Fitness and Update A_t : Use SkewPNN to classify a validation dataset using the current Bat’s hyperparameters to compute the fitness score:

$$A_i(t+1) = \lambda A_i(t),$$

where λ is the scaling factor. Using pulse rate, we let the Bats converge. Based on the highest fitness score, we identify the appropriate Bat, update \varkappa_{best} , and use it in the next iteration.

5. Stopping Criterion: We stop the algorithm when a maximum number of iterations or a satisfactory fitness score is reached.

Thus, BA-SkewPNN is well-suited for hyperparameter tuning and handles nonlinear hyperparameter space. This results in the ‘best’ values of σ and α that optimize the fitness function to improve the performance of the SkewPNN algorithm. The structure of the proposed models is illustrated in Figs. 1 and 2.

Remark 2. Advantages of our proposed methods over traditional PNN and BA-PNN: *SkewPNN and BA-SkewPNN algorithms modify the kernel used in the pattern layer of PNN. Instead of using a symmetric Gaussian kernel, a skew-normal kernel is applied to (a) model asymmetric distributions and (b) provide greater flexibility in capturing patterns in complex datasets. By tweaking α and σ , SkewPNN can enhance the influence of the underrepresented classes in the imbalanced datasets. Like PNN, SkewPNN retains its probabilistic framework, making it interpretable and robust for decision-making. In BA-SkewPNN, since we use the bio-inspired optimization algorithm for parameter estimation, this may result in improved accuracy as compared to SkewPNN for real-data applications.*

Remark 3. Limitations of the proposed methods: *Like PNN, SkewPNN presented in this study struggles with large datasets due to its reliance on storing all training samples. SkewPNN requires more memory than some of the statistical classifiers during inference because all training samples are stored in it. SkewPNN may also struggle with high-dimensional datasets. On the other hand, for very small datasets, the added flexibility of the skewness parameter in BA-SkewPNN can sometimes lead to an overfitting problem because of the usage of BA. This usually happens when we run BA for too many iterations, increasing the likelihood of overfitting by narrowing the search space too aggressively. However, we prevent this in BA-SkewPNN by using k -fold cross-validation and early stopping criteria to prevent excessive tuning.*

3.3. Implementations of Algorithm 1 and 2

A rigorous evaluation was conducted employing the 10-fold cross-validation technique to gauge the models’ efficacy. This approach partitions the dataset into ten subsets, utilizing nine subsets for training and one for validation in each iteration. Such an approach offers a robust assessment by reducing the risk of overfitting and enhancing generalization because the model is trained and validated across diverse data segments, maximizing the utilization of available information. The training and testing datasets undergo normalization through z-score normalization. Subsequently, SkewPNN is executed, with the notable modification of substituting the Gaussian kernel with the skew-normal kernel within the proposed framework. The estimation of hyper-parameters is facilitated by the BA, which integrates a unique fitness function encompassing the maximization of the summation of accuracy, AUC-ROC, and F1-score. We delved into diverse configurations of the model’s pattern layer. Within this stratum, the PDF of each class is computed to ascertain the probability of an input instance’s association with each class. For every PDF, hyper-parameters are derived via two distinct methodologies, applied to both the Gaussian and the skew-normal kernels. In the former approach, the hyper-parameters maintain uniformity across all patterns in the pattern layer. In the latter approach, however, the hyper-parameters vary for each pattern. In this context, using a population-based heuristic algorithm significantly aids in calculating distinct values for different patterns. This is because such algorithms, like the Bat optimization technique used in our study, can systematically explore the parameter space, adapting to the unique characteristics of each pattern. By allowing hyper-parameters to vary individually, the algorithm optimizes their values in alignment with the specific requirements and complexities of each pattern, ultimately enhancing the model’s adaptability and performance.

3.4. Computational Complexity

Computational complexity is a crucial indicator for measuring the efficiency of algorithms. Following the complexity analysis of several imbalanced classifiers done in the past literature [55, 57, 56], we calculate the

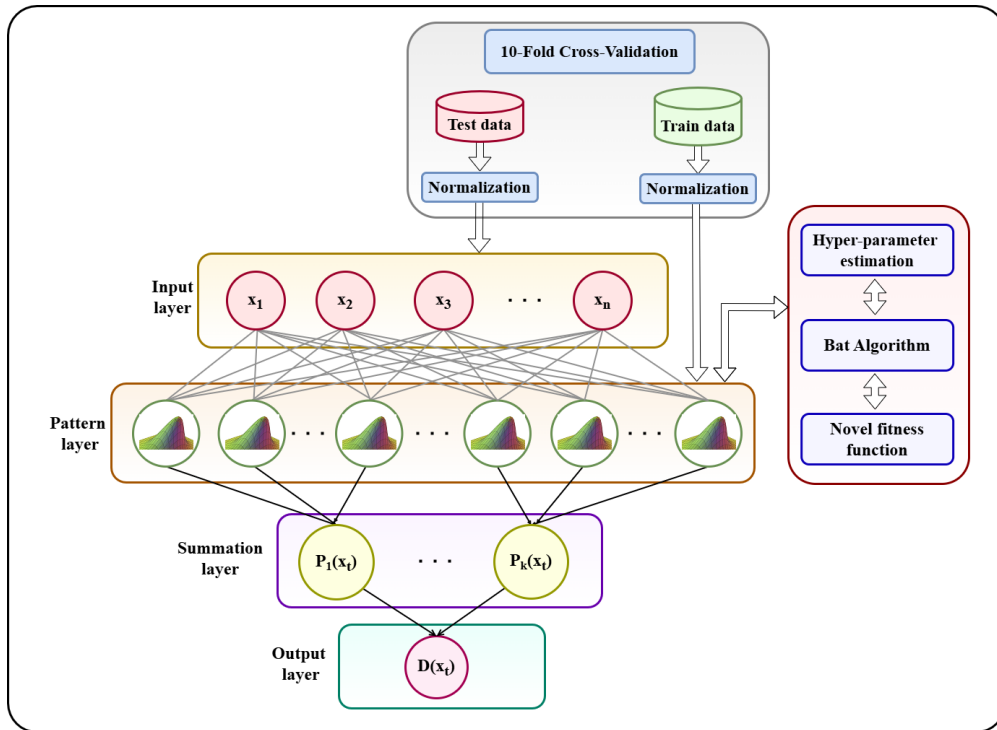


Figure 1: Schematic representation of the proposed SkewPNN and BA-SkewPNN architectures.

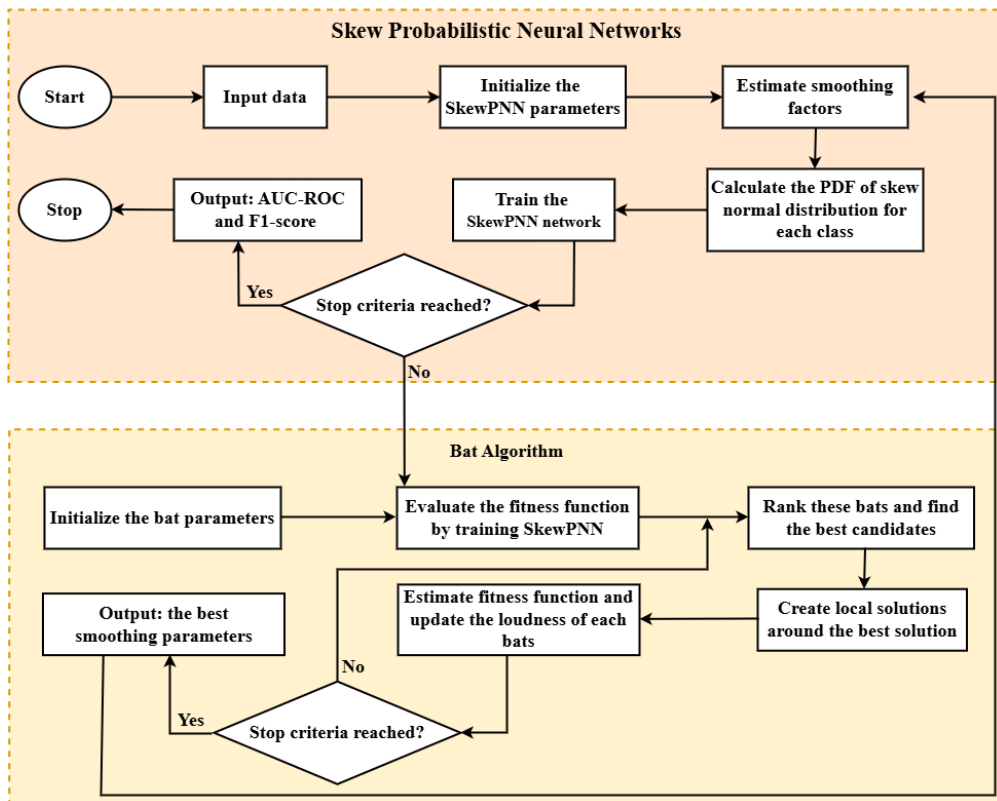


Figure 2: Workflow diagram of the proposed SkewPNN and BA-SkewPNN frameworks.

computational complexity of the proposed models. SkewPNN consists of four layers, just like PNN. The attributes of an input vector \mathbf{x} of dimension d comprise the first input layer of the model. The second layer is the pattern layer, composed of as many neurons as training data. This layer applies the kernel to the input defined in Eqn. (10). The output of the pattern neurons is fed forward to the summation layer that actually gets the average of the output of the pattern units for each class. Suppose there are J neurons in the summation layer, with each j^{th} node acquiring signals from the neurons of the j^{th} class. Finally, the decision layer declares the class assigned to the input vector based on the unit with maximum output from the summation layer. Now, we analyze the computational complexity of the proposed method and compare it with that of PNN and ANN models. Before starting that, we define the Big- \mathcal{O} notation used to describe an algorithm's performance complexity (describing the worst-case scenarios in terms of time or space complexity). Although Big- \mathcal{O} is used to compare the efficiency of various algorithms, they only describe these asymptotic behaviors (not the exact value).

Definition 1. Given two functions $f(n)$ and $q(n)$, we say that $f(n)$ is $\mathcal{O}(q(n))$ if there exist constants $e > 0$ and $n_0 \geq 0$ such that $f(n) \leq eq(n)$ for all $n \geq n_0$.

The computational complexity for the training phase in the pattern layer is $\mathcal{O}(N(d+K))$, where N is the number of training samples, d is the dimension of the input feature space and K accounts for the computational cost of $\Phi(\cdot)$. In the summation layer, the computational complexity is $\mathcal{O}(CN)$, where C is the total number of classes. Therefore, the overall computational complexity for SkewPNN is $\mathcal{O}(N(d+K))$ with the dominant term being the kernel computation, whereas, for PNN with Gaussian kernel, the complexity is $\mathcal{O}(Nd)$ for the training phase. For PNN, the total complexity for the distance calculation step is $\mathcal{O}(Nd)$, the complexity of the Gaussian kernel function is constant, and the summation layer remains $\mathcal{O}(CN)$ operation for C classes. Therefore, the overall complexity for classifying a single input vector is $\mathcal{O}(Nd)$ as Nd dominates for large d or N . Adding the skewness parameter α increases the complexity of model selection. However, the inference complexity for the traditional neural network with two hidden layers is $\mathcal{O}(N(d+N))$, much higher than SkewPNN. This is because the training is instantaneous in PNN and SkewPNN compared to the traditional neural network, which uses iterative gradient descent. For the prediction phase having M test samples, the complexity for PNN is $\mathcal{O}(MNd)$, whereas for SkewPNN, it is $\mathcal{O}(MN(d+K))$. BA-SkewPNN has higher training complexity as compared to SkewPNN due to hyperparameter tuning, which is $\mathcal{O}(TBPN(d+K))$, where T is the number of iterations for B Bats for P number of cross-validation. However, the computational complexity of SkewPNN and BA-SkewPNN is much lower than that of modern deep learning methods.

3.5. Consistency

The Parzen window estimator [62] for the PDF is expressed in Eqn. (2). K represents the kernel function, which, in our case, is the skew-normal kernel function. Here, $h(n)$ approaches zero as the data points increase. It is chosen in a way that decreases the width of the window, allowing for more localized estimation as the dataset size grows. The specific choice of $h(n)$ can depend on the problem and the characteristics of the data. The standard way to define consistency is that the expected error gets smaller as the estimates are based on a larger dataset. This is of particular interest since it will ensure that the true distribution will be approached in a smooth manner [62]. Conditions under which this happens for the density estimates are given by the following theorem:

Theorem 1. Suppose $K(x; \xi, \sigma^2, \alpha)$ (as in Eqn. 9) is a Borel function satisfying the conditions:

$$(A1) \quad \sup_{-\infty < x < \infty} |K(x; \xi, \sigma^2, \alpha)| < \infty,$$

$$(A2) \quad \int_{-\infty}^{\infty} |K(x; \xi, \sigma^2, \alpha)| dx < \infty,$$

$$(A3) \quad \lim_{x \rightarrow \infty} |xK(x; \xi, \sigma^2, \alpha)| = 0,$$

$$(A4) \quad \int_{-\infty}^{\infty} K(x; \xi, \sigma^2, \alpha) dx = 1,$$

along with the conditions in Eqn. (2) and Eqn. (3), then the estimate $f_n(x)$ is consistent in quadratic mean in the sense that

$$\mathbb{E}|f_n(x) - g(x)| \rightarrow 0 \text{ as } n \rightarrow \infty.$$

Proof. To show that $K(x; \xi, \sigma^2, \alpha)$ satisfying (A1) with skew-normal kernel density, we need to find the mode of the skew-normal distribution. For that, we establish the following result on log-concavity; that is, the logarithm of its density is a concave function [10].

Proposition 1. *The distribution $K(x; \xi, \sigma^2, \alpha)$ in SkewPNN is log-concave.*

Proof. It suffices to prove this for the case when $\xi = 0$ and $\sigma^2 = 1$ since a change of location and scale do not alter the property. To prove that $\log K(x; \xi, \sigma^2, \alpha)$ is a concave function of x , it is sufficient to show that the second derivative of $\log K(x; \xi, \sigma^2, \alpha)$ is negative for all x , following [10]:

$$\frac{d^2}{dx^2} \log K(x; \xi, \sigma^2, \alpha) = -1 + \frac{-\alpha^2 \phi(\alpha x)}{\Phi(\alpha x)} \left[\frac{\phi(\alpha x)}{\Phi(\alpha x)} + \alpha x \right]. \quad (11)$$

To show that the R.H.S. of Eqn. (11) is negative, it is sufficient to show that $B(\alpha x) = \left\{ \frac{\phi(\alpha x)}{\Phi(\alpha x)} + \alpha x \right\}$ is positive for all αx since $\phi(\alpha x)$ and $\Phi(\alpha x)$ are positive for all x .

Case I: If $\alpha x \geq 0$, then $B(\alpha x)$ is clearly positive.

Case II: If $\alpha x < 0$, let $v = -\alpha x$.

Then $\phi(\alpha x) = \phi(-\alpha x) = \phi(v)$ and $\Phi(\alpha x) = 1 - \Phi(-\alpha x) = 1 - \Phi(v)$. Therefore, we get

$$B(\alpha x) = \frac{\phi(v)}{1 - \Phi(v)} - v = r(v) - v,$$

where $r(v)$ is the failure rate of a standard normal random variable. Since it is known (see [8]) that $r(v) > v$ for all v , the assertion is proved. \square

Hence, it is evident that the mode is unique. An interesting observation for the $K(x; \xi, \sigma^2, \alpha)$ is that the unimodality holds (univariate case), which coincides with the log-concavity of the distribution. We denote by $\xi + \sigma m_0(\alpha)$ the mode of the skew-normal distribution. For any general α , no explicit expression of $m_0(\alpha)$ is available and can be done using any iterative method such as Newton-Raphson numerical optimization method. However, the authors in [10] obtained a simple and practically accurate approximation as given below:

$$m_0(\alpha) \approx \mu_z - \frac{\gamma_1 \sigma_z}{2} - \frac{\text{sgn}(\alpha)}{2} \exp\left(-\frac{2\pi}{|\alpha|}\right),$$

where $\mu_z = \sqrt{\frac{2}{\pi}}\delta$ and $\sigma_z = \sqrt{1 - \mu_z^2}$. In addition, the authors in [10] obtained via numerical simulation that the mode occurs at $\alpha \approx 1.548$, $\delta = 0.8399$, where its value is 0.5427. Therefore, the maximum value of the $K(x; \xi, \sigma^2, \alpha)$ is finite.

(A2) and (A4) are trivially satisfied as $K(x; \xi, \sigma^2, \alpha)$ is a PDF of the skew-normal distribution as defined in Eqn. (9).

(A3) To show the limiting condition, we need the existence of the expectation.

$$\mathbb{E}_{K(x; \xi, \sigma^2, \alpha)}[X] = \lim_{u \rightarrow \infty} \int_{-\infty}^u x K(x; \xi, \sigma^2, \alpha) dx = \int_{-\infty}^{\infty} x K(x; \xi, \sigma^2, \alpha) dx < \infty.$$

Since [8] derived the expression for the mean of skew-normal density function as follows: If $Y \sim SN(\xi, \sigma^2, \alpha)$,

then $\mathbb{E}[Y] = \xi + \sigma\sqrt{\frac{2}{\pi}}\delta$, where $\delta = \frac{\alpha}{\sqrt{1+\alpha^2}}$ for the univariate case and it is well defined. Now, for $u \geq 0$

$$\int_u^\infty xK(x; \xi, \sigma^2, \alpha)dx \geq u \int_u^\infty K(x; \xi, \sigma^2, \alpha)dx = u [1 - K_v(u; \xi, \sigma^2, \alpha)],$$

where $K_v(u; \xi, \sigma^2, \alpha)$ is the CDF of skew-normal kernel used in SkewPNN. Therefore, it follows that

$$\lim_{u \rightarrow \infty} \left[\mathbb{E}_K [X] - \int_{-\infty}^\infty xK(x; \xi, \sigma^2, \alpha)dx \right] = \lim_{u \rightarrow \infty} \int_u^\infty xK(x; \xi, \sigma^2, \alpha)dx = 0$$

as in the limit, the term $\int_{-\infty}^u xK(x; \xi, \sigma^2, \alpha)dx$ approaches to the expectation. By the inequality and the non-negativity of the integrand, we have the main result. Parzen [62] proved that the estimate $f_n(x)$ is consistent in quadratic mean if conditions (A1)-(A4) are met, which satisfies in this case. \square

Remark 4. *Similar to PNN, SkewPNN also approaches to Bayes optimal classification as the training set size increases.*

4. Experimental Analysis

In this section, we examined the effectiveness of our proposals on both synthetic and real-world datasets. First, we validate our proposed method on toy datasets to show the impact of the proposed mechanisms on finding smooth decision boundaries. Furthermore, numerical experiments were also conducted on real-world datasets collected from various applied fields.

4.1. Experimental Setting

In real-world data experiments, the proposed algorithmic-level solutions, namely SkewPNN and BA-SkewPNN, were compared with 16 competitive classification methods, of which 3 are data-level and 13 are algorithm-level approaches. A detailed description of these competing methods is presented in Table 2. For these existing methods, we followed the standard implementations with the default parameter settings as described in the references mentioned in Table 2. The performance of the traditional classifiers is usually measured based on classification accuracy. Although it is beneficial in balanced classification, it is inappropriate for imbalanced classification scenarios due to its preference for majority classes [72, 2, 29]. A recent study [59] showed that the area under the precision-recall curve (AUPRC) is not an appropriate performance measure in cases of class imbalance. Theoretical and empirical findings of [59] showed that AUPRC could be a harmful metric since it favors model improvements in sub-populations with more frequent majority class labels, heightening algorithmic disparities. Based on these insights, we carefully selected two evaluation indices for evaluating the experimental results, following [20, 21, 30]. Hence, we adopted two popularly used performance metrics for comparing state-of-the-art methods with our proposed models that can balance the performance between the majority and minority classes: F1 score (F1) and area under the receiver operating characteristic curve (AUC-ROC), following [20, 21, 30, 3, 75]. F1 is one of the most popular criteria for evaluating the classification accuracy of imbalanced data, which is the harmonic average of precision and recall [66]. F1 ranges between 0 and 1. The higher the F1, the better the classification effect for imbalanced data scenarios. This metric is particularly valuable when achieving a trade-off between accurate identification and minimizing false positives is essential. Another index used to measure the classification effect of imbalanced data is the area under the curve (AUC) of the receiver operating characteristic (ROC). The AUC-ROC serves as a critical metric for assessing the effectiveness of classifiers in distinguishing between positive (majority) and negative (minority) classes [47]. It visually illustrates the classifier’s performance by plotting *sensitivity* against $1 - \textit{specificity}$ at various thresholds, offering a consistent measure of the classifier’s ability to prioritize positive instances over negatives, regardless of the threshold used. Here, sensitivity, also referred to as recall, quantifies the proportion of actual positives correctly predicted by the classifier. In

contrast, specificity measures the proportion of actual negatives correctly identified by the classifier. Precision denotes the ratio of true positive predictions to all predicted positives, while sensitivity measures the proportion of true positive predictions among actual positives. Hence, the higher the value of AUC-ROC, the better the overall classification effect.

4.2. Experiments on Simulated datasets

This section provides a comprehensive analysis of the classification performance of the proposed SkewPNN model and two baseline frameworks using synthetic datasets generated with the `scikit-learn` and `imbalanced-learn` libraries in Python [54]. This analysis aims to demonstrate the distinct decision boundaries produced by these classifiers. We use three synthetic datasets to evaluate the performance of classification algorithms under varying levels of class imbalance. The half-moon dataset is generated using the `make_moons` function from the `scikit-learn` library, representing two interleaving half-circles. The concentric circles dataset is created using the `make_circles` function, comprising observations falling in concentric circles. Finally, an intertwined spiral dataset is simulated, representing two-dimensional points arising from a complex interaction of two spirals. In total, 714 observations are generated across these datasets, with Gaussian noise (standard deviation = 0.35) added to increase variability. To assess the impact of varying class imbalance, three setups are used where the imbalanced ratio (IR), the proportion of majority over minority samples, are set to 4.0, 9.0, and 19.0. In all experiments, 80% of the data samples are allocated for training, while the remaining 20% are reserved for testing the classifiers' performance. For evaluation, we compare the decision boundaries of the proposed SkewPNN method against those of the HDDT and PNN classifiers. The hyperparameter values are set as $\sigma = 0.2$ and $\alpha = -2$ for the SkewPNN model, for the HDDT the maximum depth of the tree is 5, and for PNN $\sigma = 0.1$. Figs. 3, 4, and 5 showcase the decision boundaries of the classification algorithms for the half-moon, concentric circles, and intertwined spiral datasets, respectively. As depicted in the plots, the SkewPNN model can correctly classify most of the observations and achieves the highest AUC-ROC (reported in the lower-right corner of each subplot) compared to the baseline approaches. These results affirm that the SkewPNN framework effectively handles complex data structures with nonlinear manifolds and accurately classifies both majority and minority samples across datasets with varying class imbalances. Moreover, the plots show that the HDDT-generated decision boundaries are axis-parallel lines (non-smooth), whereas SkewPNN-generated decision boundaries are very smooth. This outcome demonstrates that the proposed approach is well-suited for addressing highly imbalanced data structures.

4.3. Experiments on Real-world datasets

This section assesses the performance of the proposed algorithms for classifying real-world datasets with balanced and imbalanced class distribution. The following subsections describe the datasets used in our analysis, summarizes the performance of the proposed approaches with state-of-the-art classification methods, and evaluates the statistical significance of the performance improvements.

4.3.1. Datasets

To show the effectiveness of our proposed methods, we employed 35 datasets chosen from various fields like biology, medicine, business, and finance. Table 1 groups the datasets into two categories: Imbalanced datasets and Balanced datasets. These datasets are collected from two popular public sources such as the UCI Machine Learning Repository [31] and KEEL Imbalanced Datasets [5]. The imbalanced ratio (IR) between the samples of majority and minority classes is displayed in Table 1. By definition, a higher value of IR indicates the dataset is highly imbalanced. Following [30, 3, 75, 6], we selected 20 imbalanced datasets from KEEL where the IR ranges between 2.49 and 72.69. We also selected the balanced datasets, following [87, 3] from UCI, where the IR is close to 1. These 35 datasets also vary in terms of the number of features from 3 to 100 and the number of samples from 106 to 5472, following [30]. Out of the 35 datasets, we consider almost 25% of the datasets as multiclass data to show the strength of our proposed methods in multiclass

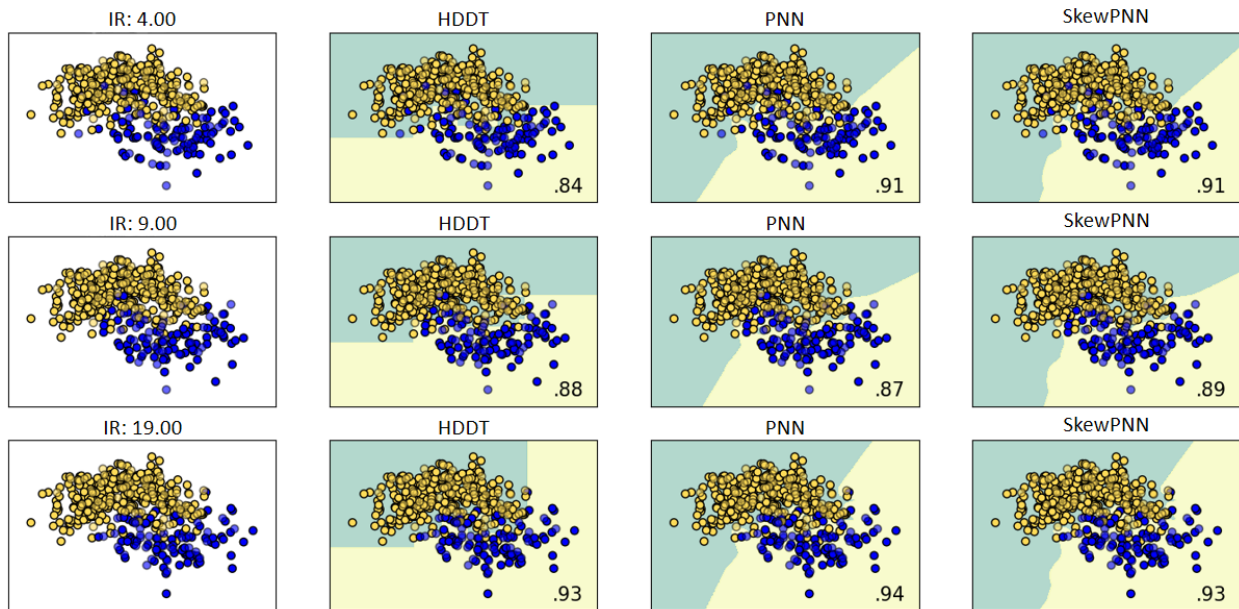


Figure 3: Comparison of HDDT, PNN, and SkewPNN classifiers on the synthetically generated half-moon dataset. Training points are displayed in solid colors, while testing points are shown with semi-transparency. The decision boundaries generated by the respective classifiers separating the two classes are depicted by green-shaded regions in subplots. The AUC-ROC score for the test set is presented in the lower-right corner of each plot.

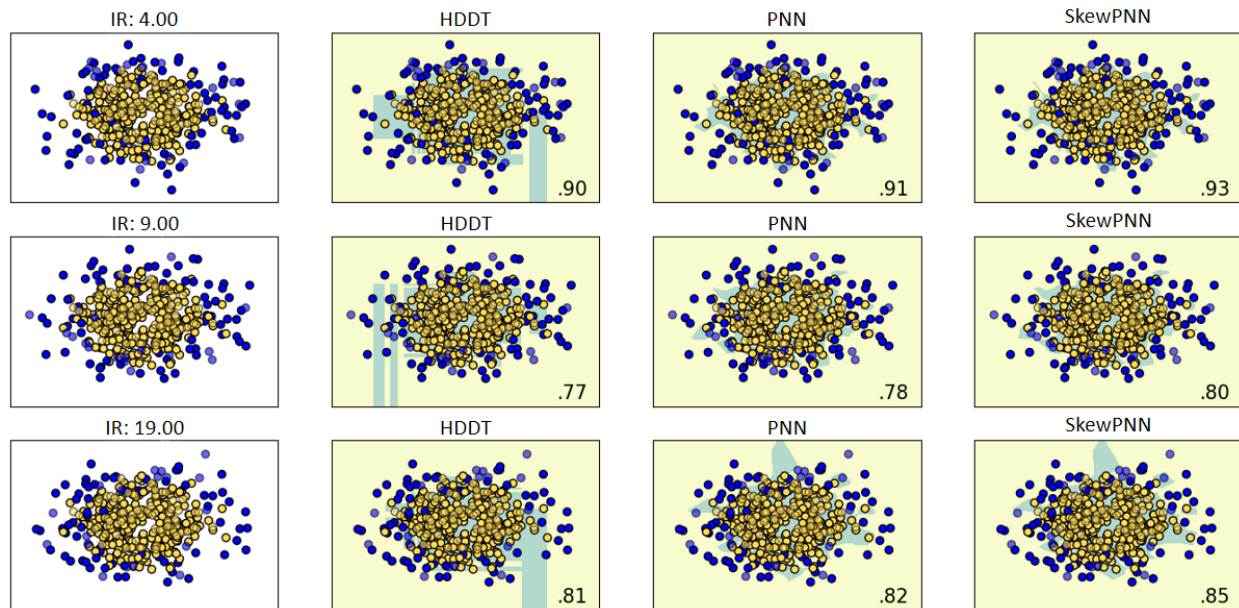


Figure 4: Comparison of HDDT, PNN, and SkewPNN classifiers on the synthetically generated concentric circles dataset. Training points are displayed in solid colors, while testing points are shown with semi-transparency. The decision boundaries generated by the respective classifiers separating the two classes are depicted by green-shaded regions in subplots. The AUC-ROC score for the test set is presented in the lower-right corner of each plot.

scenarios. The number of features ranges between 5 and 90, while the number of samples lies between 132 and 1728 for the multiclass datasets considered in this study.

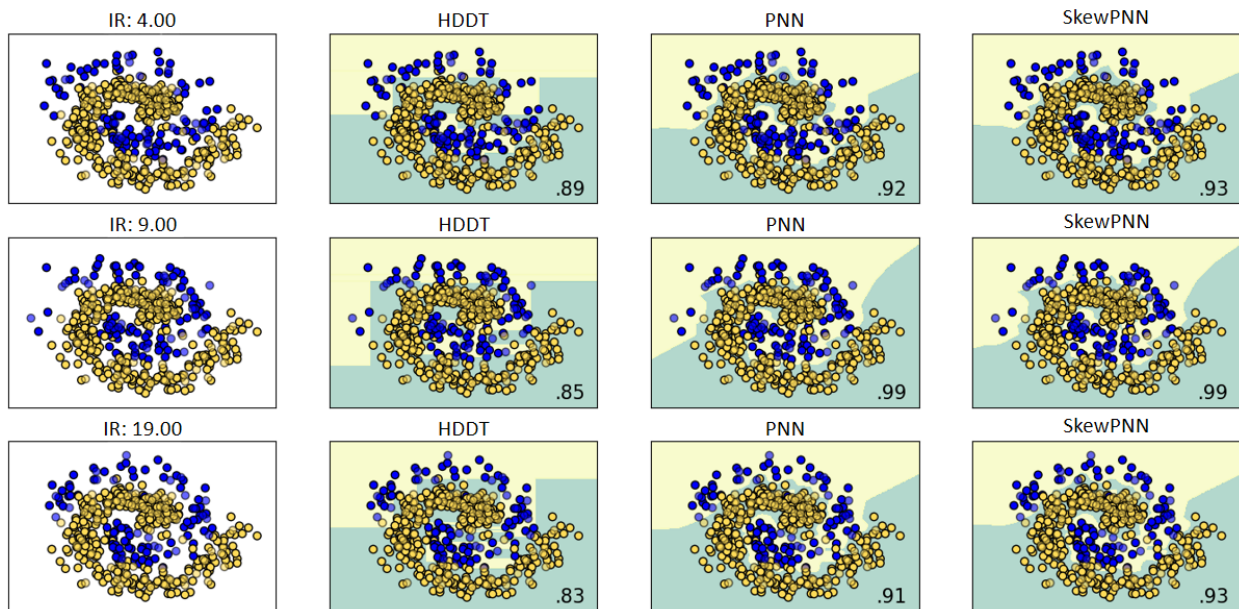


Figure 5: Comparison of HDDT, PNN, and SkewPNN classifiers on the synthetically generated intertwined spiral dataset. Training points are displayed in solid colors, while testing points are shown with semi-transparency. The decision boundaries generated by the respective classifiers separating the two classes are depicted by green-shaded regions in subplots. The AUC-ROC score for the test set is presented in the lower-right corner of each plot.

Table 1: List of Imbalanced datasets and Balanced datasets utilized in experimentation.

Sr. No.	Imbalanced Datasets	No. of Samples	No. of Attributes	No. of Classes	IR	Sr. No.	Balanced Datasets	No. of Samples	No. of Attributes	No. of Classes	IR
ID1	ecoli-0-1-4-7 vs 2-3-5-6	336	7	2	15.80	BD1	heart-c	1025	13	2	1.05
ID2	haberman	306	3	2	2.77	BD2	pima	768	8	2	1.86
ID3	vehicle3	846	18	2	2.99	BD3	tic-tac-toe	958	9	2	1.88
ID4	yeast-0-3-5-9 vs 7-8	506	8	2	9.12	BD4	australian	690	14	2	1.24
ID5	yeast-2 vs 4	514	8	2	9.07	BD5	bupa	345	6	2	1.37
ID6	page-block	5472	10	2	8.78	BD6	crx	690	15	2	1.24
ID7	abalone-20 vs 8-9-10	1916	8	2	72.69	BD7	ion	351	33	2	1.78
ID8	abalone9-18	731	8	2	16.40	BD8	hill valley	606	100	2	1.02
ID9	yeast4	1484	8	2	28.09	BD9	monks-2	432	6	2	1.11
ID10	Ecoli-0-2-3-4 vs 5	202	7	2	9.10	BD10	spect-f	80	44	2	1.00
ID11	glass-0-1-4-6 vs 2	205	9	2	11.05	BD11	wisconsin	683	9	2	1.85
ID12	appendicitis	106	7	2	4.07	BD12	tae	151	5	3	1.06
ID13	car-vgood	1728	6	2	25.58	BD13	wine	178	13	3	1.47
ID14	transfusion	748	4	2	3.20	BD14	hayes-roth	132	5	3	1.70
ID15	lipid-indian-liver	583	10	2	2.49	BD15	movement_libras	360	90	15	1.00
ID16	car-good	1728	6	4	18.61						
ID17	dermatology-6	358	34	6	5.55						
ID18	flare-F	1066	11	6	7.69						
ID19	new-thyroid	215	5	3	5.00						
ID20	DataUserMod	258	5	4	3.67						

4.3.2. Analysis of Real-world Datasets

To assess the efficacy of the proposed SkewPNN and BA-SkewPNN, we implemented them on datasets characterized by balanced and imbalanced data distributions, as detailed in Table 1. Through a series of meticulously designed experiments on these standardized datasets, we systematically compared the performance of our proposed methods against a comprehensive array of techniques for class-imbalanced (also balanced) learning. Our methodology commenced with the random shuffling of observations within each dataset, followed by the application of z-score normalization to ensure uniformity. Subsequently, we conducted 10-fold cross-validation, employing distinct and randomly generated training and test sets for each iteration. Moreover, our assessment encompassed a comprehensive comparative analysis between our pro-

Table 2: List of classifiers utilized in experimental evaluation.

Approaches	Methods	Abbreviations	Key Aspects	Publication Year
Data-Level	Synthetic Minority Oversampling TEchnique + CART [23]	SC	Oversampling Method	2002
	Synthetic Minority Oversampling TEchnique [65] with boosting + CART	SWBC	Oversampling with Boosting Approach	2022
	Generalized tHreshOld ShifTing + RF [34]	GHOST	Thresholding Method	2021
Algorithm-Level	Decision Tree [17]	DT	Tree-based Classifiers	1984
	Neural Network [64]	NN		1994
	Surface-to-Volume Ratio Tree [87]	SVRT		2023
	Hellinger Distance Decision Tree [27]	HDDT		2012
	Inter-node HDDT [3]	iHDDT		2019
	Random Forest [16]	RF	Ensemble Learning Methods	2001
	Ada Boost [38]	AB		1995
	Extreme Gradient Boosting [25]	XGB		2015
	Imbalanced XG Boost [73]	IXGB		2020
	Hellinger Distance Random Forest [70]	HDRF		2015
	Hellinger Net [20]	HNet	Neural Network Classifiers	2020
	Classical PNN [68]	PNN		1990
Bat Algorithm based PNN [78]	BA-PNN	2019		
Skew-Normal PNN	SkewPNN	Proposed		
Bat Algorithm based Skew-Normal PNN	BA-SkewPNN	Proposed		

posed classifiers and a range of benchmark methods. This empirical evaluation allowed us to assess an in-depth analysis of performance using key metrics such as AUC-ROC and F1-score.

To implement the conventional PNN where the Gaussian kernel is employed, the smoothing parameter (σ) was systematically varied across the range of 0.01 or 0.1 till approximate constant (either 1 or 10), with increments of 0.05 or 0.1 for all samples. Subsequently, we explored an alternative approach. In this variant, we integrated the Bat algorithm to dynamically assign optimal and distinct smoothing parameters for each sample during the PDF calculations. This model, denoted as BA-PNN, operated with two distinct smoothing parameter intervals: [0.01, 1.0) and [0.1, 1.0). Moving forward, we conducted experiments utilizing our proposed SkewPNN and BA-SkewPNN. In the SkewPNN, we leveraged the skew-normal kernel to estimate the values within pattern layers. We choose the skewness parameter for SkewPNN from a pre-specified range of [-6, 6]. Similarly, the smoothing parameter is chosen across samples, ranging from 0.01 or 0.1 to approximate constant (either 1 or 10), with intervals of 0.05 or 0.1. In the case of the BA-SkewPNN model, the BA algorithm was employed to assign the optimal and diverse smoothing parameters for the PDF calculations across all the samples. Likewise, two distinct intervals were maintained for selecting smoothing parameters: [0.01, 1.0) or [0.1, 1.0). Notably, the fitness function remained consistent for both BA-PNN and BA-SkewPNN.

Tables 3 and 4 summarize the performance of the proposed methods and the state-of-art frameworks for classifying the imbalanced and balanced datasets based on the AUC-ROC and F1 metrics, respectively. These tables represent the mean (standard deviation) values of the accuracy measures obtained through 10-fold cross-validation. For the imbalanced datasets, the proposed BA-SkewPNN model achieves the highest AUC-ROC values in 14 out of 20 cases and the best F1 scores in 9 datasets. Similarly, the SkewPNN framework demonstrates excellent performance over state-of-the-art classifiers across several real-world datasets, as evident from its AUC-ROC and F1 metrics. Among the competing models, HNet achieves the highest classification accuracy for the page-block and Ecoli-0-2-3-4 vs 5 datasets. For the imbalanced multiclass datasets, the proposed approaches either outperform or perform comparably to the baseline frameworks. Specifically, for the dermatology-6 and flare-F datasets, the SkewPNN, BA-SkewPNN, PNN, and BA-PNN models provide the most accurate results. The empirical evaluations on the real-world balanced datasets further underscore the superiority of the proposed BA-SkewPNN framework. In terms of the AUC-ROC metric, BA-SkewPNN achieves the highest accuracy in 6 out of 15 datasets, followed by SkewPNN, GHOST, and XGB models. Similarly, the F1 metrics reveal a consistent trend, with BA-SkewPNN excelling in 6 out of 20 datasets, followed by SkewPNN, PNN, and XGB. For the balanced multiclass datasets, the BA-SkewPNN model outperforms the state-of-the-art classifiers in 3 out of 4 cases. As outlined in Remark 3, here, we also experimentally observed that SkewPNN and BA-SkewPNN could not showcase the best possible performance as compared to state-of-the-art methods in Table 3 and 4 when the curse of many dimensions occurred. As the number of input features increases, the estimator of PDF becomes difficult in complex and high-dimensional spaces. Also, to some extent, large datasets contribute to the failure cases of our proposed methods in Table 3

Table 3: Experimental results encompassing AUC-ROC and F1-score (mean and standard deviation in bracket) analyses conducted on imbalanced datasets listed in Table 1. The highest value of the metrics for a particular dataset is highlighted in **bold**.

Data	Measure	DT	NN	AB	RF	SC	SVRT	HDDT	HDRF	XGB	IXGB	HNet	iHDDT	GHOST	SWBC	PNN	BA-PNN	SkewPNN	BA-SkewPNN
ID1	AUC-ROC	0.819 (0.141)	0.859 (0.125)	0.818 (0.108)	0.820 (0.134)	0.765 (0.102)	0.862 (0.066)	0.787 (0.123)	0.803 (0.145)	0.943 (0.055)	0.968 (0.030)	0.900 (0.056)	0.509 (0.041)	0.900 (0.075)	0.861 (0.119)	0.908 (0.118)	0.921 (0.012)	0.933 (0.132)	0.980 (0.047)
	F1	0.622 (0.204)	0.756 (0.193)	0.716 (0.166)	0.726 (0.211)	0.612 (0.161)	0.737 (0.087)	0.601 (0.203)	0.700 (0.244)	0.526 (0.192)	0.893 (0.101)	0.889 (0.078)	0.000 (0.000)	0.689 (0.146)	0.753 (0.170)	0.744 (0.318)	0.857 (0.034)	0.774 (0.332)	0.881 (0.255)
ID2	AUC-ROC	0.540 (0.108)	0.579 (0.095)	0.594 (0.096)	0.555 (0.077)	0.582 (0.069)	0.506 (0.016)	0.552 (0.087)	0.546 (0.127)	0.548 (0.076)	0.513 (0.060)	0.550 (0.060)	0.492 (0.021)	0.626 (0.057)	0.560 (0.074)	0.588 (0.061)	0.595 (0.123)	0.588 (0.060)	0.665 (0.118)
	F1	0.312 (0.167)	0.304 (0.207)	0.353 (0.187)	0.300 (0.140)	0.310 (0.096)	0.449 (0.017)	0.332 (0.156)	0.275 (0.235)	0.308 (0.167)	0.244 (0.118)	0.294 (0.032)	0.045 (0.071)	0.444 (0.090)	0.344 (0.117)	0.402 (0.085)	0.401 (0.174)	0.403 (0.079)	0.513 (0.136)
ID3	AUC-ROC	0.667 (0.076)	0.598 (0.057)	0.637 (0.056)	0.637 (0.048)	0.629 (0.044)	0.714 (0.047)	0.685 (0.092)	0.666 (0.064)	0.648 (0.064)	0.662 (0.055)	0.662 (0.027)	0.533 (0.024)	0.693 (0.042)	0.664 (0.041)	0.709 (0.050)	0.712 (0.040)	0.711 (0.058)	0.718 (0.051)
	F1	0.499 (0.114)	0.344 (0.146)	0.438 (0.111)	0.433 (0.154)	0.396 (0.063)	0.559 (0.078)	0.528 (0.062)	0.490 (0.116)	0.491 (0.109)	0.463 (0.091)	0.488 (0.045)	0.171 (0.070)	0.541 (0.065)	0.498 (0.063)	0.548 (0.056)	0.558 (0.052)	0.551 (0.065)	0.561 (0.062)
ID4	AUC-ROC	0.599 (0.062)	0.598 (0.110)	0.659 (0.128)	0.539 (0.048)	0.549 (0.067)	0.648 (0.012)	0.652 (0.102)	0.588 (0.094)	0.623 (0.101)	0.536 (0.107)	0.568 (0.027)	0.503 (0.183)	0.653 (0.078)	0.596 (0.081)	0.676 (0.081)	0.741 (0.152)	0.718 (0.104)	0.751 (0.044)
	F1	0.286 (0.134)	0.279 (0.248)	0.401 (0.278)	0.129 (0.158)	0.153 (0.094)	0.345 (0.219)	0.369 (0.171)	0.256 (0.249)	0.333 (0.212)	0.138 (0.226)	0.135 (0.079)	0.019 (0.049)	0.377 (0.133)	0.261 (0.145)	0.331 (0.146)	0.455 (0.207)	0.455 (0.194)	0.449 (0.181)
ID5	AUC-ROC	0.795 (0.104)	0.821 (0.09)	0.841 (0.103)	0.830 (0.094)	0.801 (0.070)	0.834 (0.102)	0.819 (0.109)	0.825 (0.122)	0.826 (0.095)	0.833 (0.089)	0.687 (0.034)	0.687 (0.086)	0.905 (0.048)	0.902 (0.056)	0.902 (0.093)	0.902 (0.088)	0.902 (0.088)	0.910 (0.059)
	F1	0.625 (0.166)	0.741 (0.105)	0.729 (0.154)	0.749 (0.140)	0.642 (0.101)	0.676 (0.164)	0.672 (0.195)	0.750 (0.137)	0.609 (0.124)	0.696 (0.050)	0.667 (0.170)	0.479 (0.088)	0.766 (0.085)	0.777 (0.155)	0.776 (0.155)	0.775 (0.134)	0.775 (0.077)	0.779 (0.077)
ID6	AUC-ROC	0.904 (0.028)	0.923 (0.025)	0.879 (0.035)	0.919 (0.025)	0.914 (0.019)	0.924 (0.016)	0.912 (0.030)	0.925 (0.022)	0.878 (0.028)	0.922 (0.028)	0.934 (0.008)	0.809 (0.201)	0.809 (0.021)	0.851 (0.016)	0.903 (0.050)	0.903 (0.031)	0.850 (0.052)	0.850 (0.035)
	F1	0.833 (0.029)	0.853 (0.048)	0.801 (0.043)	0.870 (0.023)	0.846 (0.023)	0.841 (0.022)	0.842 (0.044)	0.880 (0.022)	0.792 (0.036)	0.866 (0.040)	0.885 (0.011)	0.695 (0.032)	0.868 (0.024)	0.839 (0.025)	0.678 (0.054)	0.770 (0.067)	0.671 (0.057)	0.671 (0.065)
ID7	AUC-ROC	0.638 (0.124)	0.566 (0.111)	0.615 (0.125)	0.542 (0.085)	0.587 (0.095)	0.608 (0.128)	0.597 (0.075)	0.525 (0.094)	0.593 (0.092)	0.586 (0.062)	0.600 (0.008)	0.646 (0.201)	0.589 (0.021)	0.599 (0.016)	0.791 (0.120)	0.809 (0.149)	0.812 (0.128)	0.842 (0.106)
	F1	0.283 (0.260)	0.180 (0.286)	0.283 (0.289)	0.117 (0.236)	0.201 (0.106)	0.284 (0.176)	0.190 (0.246)	0.067 (0.200)	0.240 (0.253)	0.150 (0.229)	0.230 (0.183)	0.000 (0.000)	0.227 (0.172)	0.211 (0.191)	0.191 (0.067)	0.130 (0.148)	0.130 (0.089)	0.331 (0.139)
ID8	AUC-ROC	0.605 (0.104)	0.592 (0.065)	0.657 (0.107)	0.534 (0.054)	0.597 (0.100)	0.608 (0.066)	0.615 (0.061)	0.557 (0.059)	0.568 (0.138)	0.558 (0.111)	0.562 (0.016)	0.500 (0.000)	0.696 (0.075)	0.639 (0.061)	0.660 (0.184)	0.689 (0.138)	0.691 (0.148)	0.719 (0.129)
	F1	0.264 (0.208)	0.284 (0.196)	0.320 (0.259)	0.113 (0.174)	0.242 (0.112)	0.243 (0.123)	0.265 (0.118)	0.187 (0.188)	0.350 (0.282)	0.319 (0.562)	0.222 (0.055)	0.000 (0.000)	0.321 (0.127)	0.307 (0.106)	0.207 (0.132)	0.282 (0.163)	0.301 (0.171)	0.362 (0.170)
ID9	AUC-ROC	0.670 (0.130)	0.538 (0.046)	0.595 (0.085)	0.557 (0.047)	0.589 (0.092)	0.641 (0.074)	0.574 (0.107)	0.554 (0.068)	0.562 (0.083)	0.565 (0.024)	0.570 (0.054)	0.664 (0.067)	0.625 (0.056)	0.846 (0.104)	0.853 (0.113)	0.847 (0.126)	0.847 (0.140)	0.861 (0.140)
	F1	0.352 (0.249)	0.120 (0.149)	0.234 (0.165)	0.179 (0.150)	0.189 (0.113)	0.327 (0.106)	0.289 (0.197)	0.202 (0.177)	0.154 (0.219)	0.212 (0.188)	0.190 (0.078)	0.363 (0.123)	0.334 (0.121)	0.337 (0.104)	0.334 (0.081)	0.334 (0.106)	0.334 (0.100)	0.334 (0.146)
ID10	AUC-ROC	0.836 (0.167)	0.892 (0.127)	0.869 (0.172)	0.845 (0.165)	0.825 (0.101)	0.718 (0.125)	0.845 (0.165)	0.845 (0.165)	0.840 (0.157)	0.859 (0.000)	1.000 (0.000)	0.551 (0.087)	0.928 (0.052)	0.842 (0.096)	0.908 (0.113)	0.934 (0.107)	0.913 (0.174)	0.930 (0.108)
	F1	0.683 (0.302)	0.813 (0.203)	0.767 (0.327)	0.730 (0.299)	0.677 (0.121)	0.730 (0.040)	0.730 (0.299)	0.650 (0.288)	0.737 (0.000)	1.000 (0.183)	0.170 (0.096)	0.715 (0.150)	0.708 (0.256)	0.733 (0.196)	0.834 (0.067)	0.743 (0.185)	0.743 (0.185)	0.743 (0.218)
ID11	AUC-ROC	0.554 (0.171)	0.590 (0.000)	0.687 (0.119)	0.547 (0.102)	0.536 (0.141)	0.587 (0.139)	0.704 (0.182)	0.522 (0.076)	0.469 (0.071)	0.575 (0.081)	0.575 (0.007)	0.493 (0.107)	0.647 (0.130)	0.606 (0.114)	0.642 (0.145)	0.747 (0.118)	0.745 (0.118)	0.757 (0.118)
	F1	0.167 (0.342)	0.000 (0.000)	0.417 (0.359)	0.133 (0.267)	0.111 (0.212)	0.226 (0.077)	0.440 (0.325)	0.067 (0.200)	0.050 (0.150)	0.210 (0.200)	0.210 (0.037)	0.000 (0.000)	0.308 (0.212)	0.256 (0.207)	0.196 (0.216)	0.270 (0.226)	0.284 (0.225)	0.280 (0.223)
ID12	AUC-ROC	0.698 (0.139)	0.764 (0.178)	0.692 (0.183)	0.703 (0.124)	0.721 (0.095)	0.712 (0.081)	0.659 (0.181)	0.747 (0.147)	0.691 (0.188)	0.710 (0.190)	0.792 (0.081)	0.660 (0.111)	0.790 (0.113)	0.699 (0.113)	0.801 (0.128)	0.811 (0.126)	0.791 (0.148)	0.826 (0.097)
	F1	0.507 (0.243)	0.600 (0.351)	0.492 (0.302)	0.490 (0.156)	0.546 (0.156)	0.562 (0.194)	0.398 (0.357)	0.597 (0.281)	0.467 (0.356)	0.467 (0.135)	0.618 (0.207)	0.420 (0.164)	0.610 (0.174)	0.474 (0.174)	0.667 (0.174)	0.692 (0.165)	0.614 (0.209)	0.698 (0.138)
ID13	AUC-ROC	0.991 (0.025)	0.843 (0.092)	0.951 (0.055)	0.968 (0.053)	0.970 (0.040)	0.977 (0.012)	0.983 (0.031)	0.984 (0.063)	0.939 (0.100)	0.906 (0.029)	0.500 (0.000)	0.952 (0.056)	0.982 (0.024)	0.917 (0.072)	0.958 (0.155)	0.958 (0.041)	0.958 (0.041)	0.983 (0.018)
	F1	0.983 (0.034)	0.769 (0.152)	0.885 (0.098)	0.949 (0.062)	0.947 (0.049)	0.969 (0.023)	0.966 (0.041)	0.976 (0.038)	0.700 (0.053)	0.891 (0.054)	0.897 (0.000)	0.861 (0.073)	0.975 (0.032)	0.635 (0.332)	0.771 (0.246)	0.635 (0.331)	0.760 (0.234)	0.760 (0.234)
ID14	AUC-ROC	0.638 (0.064)	0.573 (0.044)	0.629 (0.074)	0.599 (0.061)	0.556 (0.049)	0.654 (0.031)	0.619 (0.066)	0.605 (0.066)	0.610 (0.064)	0.614 (0.036)	0.497 (0.020)	0.671 (0.006)	0.570 (0.034)	0.602 (0.080)	0.650 (0.219)	0.610 (0.072)	0.610 (0.072)	0.672 (0.246)
	F1	0.448 (0.087)	0.267 (0.126)	0.413 (0.157)	0.378 (0.102)	0.175 (0.073)	0.458 (0.081)	0.419 (0.097)	0.386 (0.116)	0.380 (0.118)	0.423 (0.072)	0.002 (0.038)	0.496 (0.008)	0.336 (0.071)	0.399 (0.057)	0.464 (0.107)	0.408 (0.081)	0.451 (0.081)	0.451 (0.095)
ID15	AUC-ROC	0.573 (0.084)	0.500 (0.000)	0.573 (0.035)	0.563 (0.060)	0.503 (0.052)	0.636 (0.021)	0.598 (0.076)	0.598 (0.052)	0.590 (0.054)	0.567 (0.022)	0.575 (0.038)	0.553 (0.028)	0.582 (0.056)	0.660 (0.071)	0.660 (0.080)	0.660 (0.001)	0.669 (0.001)	0.669 (0.070)
	F1	0.377 (0.123)	0.000 (0.000)	0.355 (0.050)	0.330 (0.101)	0.431 (0.032)	0.496 (0.069)	0.429 (0.102)	0.394 (0.126)	0.386 (0.088)	0.353 (0.057)	0.782 (0.028)	0.807 (0.017)	0.757 (0.030)	0.682 (0.084)	0.651 (0.122)	0.642 (0.001)	0.642 (0.001)	0.687 (0.312)
ID16	AUC-ROC	0.934 (0.051)	0.838 (0.070)	0.629 (0.095)	0.876 (0.021)	0.921 (0.021)	0.760 (0.005)	0.941 (0.045)	0.870 (0.109)	0.875 (0.067)	0.837 (0.057)	0.855 (0.048)	0.690 (0.017)	0.910 (0.025)	0.963 (0.011)	0.889 (0.065)	0.919 (0.076)	0.913 (0.063)	0.953 (0.076)
	F1	0.908 (0.078)	0.760 (0.110)	0.341 (0.221)	0.837 (0.100)	0.847 (0.010)	0.627 (0.006)	0.921 (0.078)	0.818 (0.153)	0.762 (0.088)	0.784 (0.082)	0.789 (0.074)	0.206 (0.012)	0.839 (0.028)	0.943 (0.017)	0.681 (0.166)	0.704 (0.234)	0.716 (0.181)	0.720 (0.210)
ID17	AUC-ROC	0.949 (0.091)	1.000 (0.000)	0.999 (0.004)	1.000 (0.000)	0.959 (0.016)	0.978 (0.067)	0.999 (0.004)	0.975 (0.075)	0.998 (0.004)	0.974 (0.057)	1.000 (0.000)	0.653 (0.947)	0.945 (0.040)	0.959 (0.016)	1.000 (0.			

Table 4: Experimental results encompassing AUC-ROC and F1-score (mean and standard deviation in bracket) analyses conducted on balanced datasets listed in Table 1. The highest value of the metrics for a particular dataset is highlighted in **bold**.

Data	Measure	DT	NN	AB	RF	SC	SVRT	HDDT	HDRF	XGB	IXGB	HNet	iHDDT	GHOST	SWBC	PNN	BA-PNN	SkewPNN	BA-SkewPNN
BD1	AUC-ROC	0.725 (0.073)	0.827 (0.041)	0.791 (0.058)	0.795 (0.043)	0.996 (0.008)	0.524 (0.063)	0.733 (0.044)	0.810 (0.053)	0.814 (0.065)	0.795 (0.025)	0.745 (0.028)	0.634 (0.015)	0.956 (0.006)	0.996 (0.000)	1.000 (0.000)	1.000 (0.000)	1.000 (0.000)	1.000 (0.000)
	F1	0.705 (0.069)	0.811 (0.044)	0.766 (0.049)	0.770 (0.049)	0.996 (0.008)	0.212 (0.103)	0.709 (0.077)	0.788 (0.060)	0.798 (0.059)	0.775 (0.071)	0.712 (0.031)	0.627 (0.033)	0.958 (0.014)	0.997 (0.006)	1.000 (0.000)	1.000 (0.000)	1.000 (0.000)	1.000 (0.000)
BD2	AUC-ROC	0.690 (0.056)	0.728 (0.057)	0.735 (0.046)	0.704 (0.045)	0.671 (0.035)	0.703 (0.049)	0.679 (0.055)	0.712 (0.061)	0.714 (0.048)	0.718 (0.049)	0.705 (0.025)	0.578 (0.030)	0.733 (0.029)	0.680 (0.034)	0.724 (0.068)	0.727 (0.057)	0.716 (0.048)	0.737 (0.038)
	F1	0.594 (0.074)	0.639 (0.087)	0.650 (0.069)	0.605 (0.067)	0.578 (0.044)	0.627 (0.073)	0.584 (0.067)	0.617 (0.088)	0.627 (0.063)	0.627 (0.070)	0.595 (0.036)	0.359 (0.062)	0.649 (0.038)	0.585 (0.046)	0.645 (0.084)	0.634 (0.073)	0.645 (0.060)	0.650 (0.050)
BD3	AUC-ROC	0.882 (0.036)	0.840 (0.034)	0.660 (0.061)	0.923 (0.036)	0.850 (0.027)	0.790 (0.030)	0.896 (0.034)	0.925 (0.029)	0.998 (0.005)	0.918 (0.033)	0.799 (0.021)	0.500 (0.000)	0.821 (0.024)	0.866 (0.022)	0.796 (0.070)	0.711 (0.074)	0.812 (0.078)	0.775 (0.080)
	F1	0.924 (0.021)	0.905 (0.017)	0.803 (0.046)	0.959 (0.019)	0.880 (0.020)	0.730 (0.025)	0.929 (0.024)	0.960 (0.014)	0.999 (0.002)	0.955 (0.017)	0.863 (0.012)	0.790 (0.019)	0.911 (0.011)	0.909 (0.017)	0.911 (0.084)	0.909 (0.054)	0.835 (0.060)	0.873 (0.094)
BD4	AUC-ROC	0.797 (0.042)	0.867 (0.021)	0.867 (0.022)	0.858 (0.027)	0.850 (0.000)	0.812 (0.021)	0.798 (0.038)	0.860 (0.029)	0.856 (0.025)	0.851 (0.036)	0.846 (0.013)	0.500 (0.000)	0.887 (0.002)	0.857 (0.000)	0.631 (0.067)	0.669 (0.115)	0.532 (0.032)	0.859 (0.040)
	F1	0.776 (0.046)	0.854 (0.024)	0.853 (0.025)	0.842 (0.032)	0.834 (0.000)	0.834 (0.048)	0.799 (0.046)	0.775 (0.034)	0.843 (0.031)	0.839 (0.038)	0.835 (0.014)	0.829 (0.000)	0.854 (0.005)	0.806 (0.000)	0.557 (0.090)	0.529 (0.278)	0.421 (0.049)	0.558 (0.045)
BD5	AUC-ROC	0.597 (0.075)	0.688 (0.078)	0.683 (0.063)	0.685 (0.067)	0.619 (0.057)	0.616 (0.063)	0.597 (0.058)	0.695 (0.066)	0.704 (0.093)	0.703 (0.042)	0.698 (0.028)	0.490 (0.031)	0.714 (0.053)	0.628 (0.053)	0.634 (0.091)	0.688 (0.065)	0.727 (0.070)	0.635 (0.079)
	F1	0.664 (0.069)	0.767 (0.066)	0.746 (0.046)	0.736 (0.049)	0.549 (0.072)	0.538 (0.071)	0.670 (0.051)	0.754 (0.054)	0.759 (0.075)	0.769 (0.044)	0.725 (0.028)	0.281 (0.092)	0.679 (0.056)	0.571 (0.064)	0.575 (0.171)	0.643 (0.078)	0.599 (0.087)	0.644 (0.067)
BD6	AUC-ROC	0.821 (0.048)	0.864 (0.035)	0.857 (0.037)	0.864 (0.035)	0.794 (0.032)	0.797 (0.032)	0.812 (0.058)	0.880 (0.032)	0.924 (0.055)	0.920 (0.055)	0.891 (0.013)	0.899 (0.008)	0.649 (0.019)	0.915 (0.030)	0.882 (0.063)	0.928 (0.132)	0.942 (0.066)	0.934 (0.142)
	F1	0.805 (0.052)	0.853 (0.037)	0.843 (0.042)	0.848 (0.049)	0.770 (0.041)	0.837 (0.049)	0.792 (0.066)	0.868 (0.034)	0.873 (0.058)	0.852 (0.060)	0.767 (0.015)	0.000 (0.000)	0.864 (0.021)	0.778 (0.034)	0.902 (0.092)	0.548 (0.118)	0.790 (0.097)	0.862 (0.136)
BD7	AUC-ROC	0.843 (0.043)	0.913 (0.048)	0.900 (0.073)	0.925 (0.040)	0.877 (0.032)	0.871 (0.038)	0.846 (0.061)	0.924 (0.044)	0.890 (0.017)	0.891 (0.031)	0.899 (0.011)	0.649 (0.029)	0.915 (0.037)	0.882 (0.037)	0.928 (0.043)	0.928 (0.046)	0.942 (0.043)	0.934 (0.050)
	F1	0.895 (0.031)	0.951 (0.026)	0.935 (0.050)	0.950 (0.024)	0.843 (0.024)	0.833 (0.027)	0.895 (0.042)	0.895 (0.028)	0.955 (0.008)	0.935 (0.023)	0.933 (0.009)	0.842 (0.036)	0.949 (0.022)	0.916 (0.028)	0.953 (0.039)	0.949 (0.034)	0.953 (0.039)	0.945 (0.033)
BD8	AUC-ROC	0.597 (0.040)	0.500 (0.000)	0.481 (0.061)	0.581 (0.052)	0.536 (0.041)	0.509 (0.039)	0.508 (0.032)	0.605 (0.059)	0.601 (0.044)	0.535 (0.027)	0.532 (0.039)	0.509 (0.039)	0.526 (0.043)	0.554 (0.078)	0.527 (0.063)	0.523 (0.074)	0.526 (0.030)	0.533 (0.030)
	F1	0.582 (0.076)	0.000 (0.000)	0.549 (0.065)	0.576 (0.078)	0.697 (0.050)	0.567 (0.058)	0.499 (0.167)	0.593 (0.077)	0.602 (0.066)	0.541 (0.055)	0.496 (0.003)	0.490 (0.043)	0.557 (0.044)	0.563 (0.078)	0.388 (0.095)	0.554 (0.067)	0.381 (0.203)	0.459 (0.203)
BD9	AUC-ROC	0.764 (0.117)	0.517 (0.061)	0.488 (0.050)	0.631 (0.107)	0.489 (0.087)	0.485 (0.101)	0.754 (0.103)	0.618 (0.140)	0.736 (0.159)	0.629 (0.146)	0.627 (0.045)	0.737 (0.031)	0.411 (0.033)	0.663 (0.038)	0.983 (0.025)	0.821 (0.061)	0.984 (0.025)	0.866 (0.101)
	F1	0.704 (0.137)	0.136 (0.136)	0.245 (0.114)	0.512 (0.141)	0.346 (0.101)	0.302 (0.113)	0.688 (0.121)	0.483 (0.212)	0.483 (0.188)	0.546 (0.190)	0.580 (0.073)	0.634 (0.097)	0.965 (0.027)	0.713 (0.085)	0.981 (0.027)	0.839 (0.043)	0.981 (0.027)	0.885 (0.076)
BD10	AUC-ROC	0.642 (0.127)	0.512 (0.016)	0.690 (0.087)	0.643 (0.102)	0.543 (0.084)	0.618 (0.101)	0.647 (0.100)	0.661 (0.094)	0.629 (0.108)	0.627 (0.127)	0.737 (0.048)	0.411 (0.097)	0.633 (0.080)	0.706 (0.119)	0.763 (0.102)	0.750 (0.124)	0.763 (0.109)	0.764 (0.124)
	F1	0.855 (0.055)	0.045 (0.059)	0.878 (0.032)	0.882 (0.029)	0.548 (0.109)	0.385 (0.118)	0.849 (0.056)	0.888 (0.031)	0.874 (0.085)	0.863 (0.065)	0.889 (0.017)	0.304 (0.155)	0.727 (0.049)	0.692 (0.133)	0.725 (0.166)	0.647 (0.145)	0.666 (0.179)	0.671 (0.214)
BD11	AUC-ROC	0.947 (0.022)	0.965 (0.024)	0.953 (0.023)	0.959 (0.015)	0.944 (0.024)	0.949 (0.020)	0.944 (0.024)	0.964 (0.022)	0.944 (0.024)	0.962 (0.019)	0.963 (0.004)	0.803 (0.032)	0.976 (0.013)	0.934 (0.022)	0.960 (0.032)	0.967 (0.032)	0.967 (0.024)	0.970 (0.019)
	F1	0.932 (0.029)	0.952 (0.031)	0.941 (0.032)	0.947 (0.017)	0.926 (0.030)	0.928 (0.018)	0.927 (0.029)	0.952 (0.026)	0.933 (0.022)	0.950 (0.022)	0.950 (0.005)	0.752 (0.046)	0.964 (0.018)	0.915 (0.027)	0.966 (0.027)	0.972 (0.020)	0.976 (0.016)	0.979 (0.014)
BD12	AUC-ROC	0.750 (0.083)	0.548 (0.090)	0.592 (0.103)	0.754 (0.092)	0.734 (0.064)	0.753 (0.086)	0.602 (0.029)	0.599 (0.090)	0.708 (0.086)	0.761 (0.036)	0.595 (0.049)	0.567 (0.048)	0.694 (0.066)	0.700 (0.066)	0.795 (0.202)	0.858 (0.175)	0.760 (0.241)	0.862 (0.181)
	F1	0.653 (0.109)	0.390 (0.129)	0.435 (0.153)	0.663 (0.133)	0.630 (0.086)	0.656 (0.113)	0.361 (0.051)	0.363 (0.106)	0.646 (0.114)	0.642 (0.046)	0.306 (0.044)	0.133 (0.061)	0.593 (0.058)	0.579 (0.024)	0.779 (0.224)	0.833 (0.172)	0.829 (0.171)	0.869 (0.211)
BD13	AUC-ROC	0.935 (0.039)	0.943 (0.022)	0.903 (0.048)	0.973 (0.015)	0.944 (0.032)	0.941 (0.021)	0.735 (0.023)	0.760 (0.033)	0.970 (0.010)	0.973 (0.010)	0.772 (0.015)	0.642 (0.092)	0.818 (0.129)	0.819 (0.083)	0.955 (0.083)	0.957 (0.070)	0.956 (0.082)	0.980 (0.063)
	F1	0.915 (0.051)	0.977 (0.028)	0.876 (0.064)	0.989 (0.021)	0.927 (0.042)	0.973 (0.019)	0.532 (0.015)	0.559 (0.015)	0.960 (0.018)	0.951 (0.021)	0.584 (0.184)	0.344 (0.217)	0.749 (0.163)	0.757 (0.175)	0.956 (0.078)	0.950 (0.078)	0.956 (0.078)	0.983 (0.052)
BD14	AUC-ROC	0.890 (0.063)	0.848 (0.079)	0.721 (0.055)	0.892 (0.053)	0.717 (0.053)	0.752 (0.059)	0.656 (0.030)	0.673 (0.078)	0.869 (0.024)	0.894 (0.024)	0.914 (0.069)	0.601 (0.103)	0.823 (0.109)	0.829 (0.110)	0.570 (0.139)	0.650 (0.118)	0.704 (0.173)	0.782 (0.175)
	F1	0.865 (0.081)	0.814 (0.102)	0.556 (0.075)	0.866 (0.080)	0.820 (0.063)	0.762 (0.033)	0.456 (0.074)	0.480 (0.042)	0.844 (0.092)	0.872 (0.028)	0.895 (0.184)	0.344 (0.138)	0.759 (0.149)	0.775 (0.149)	0.568 (0.166)	0.668 (0.124)	0.668 (0.212)	0.736 (0.212)
BD15	AUC-ROC	0.573 (0.097)	0.620 (0.019)	0.780 (0.082)	0.738 (0.082)	0.756 (0.041)	0.850 (0.049)	0.608 (0.043)	0.727 (0.101)	0.739 (0.041)	0.723 (0.076)	0.748 (0.018)	0.627 (0.132)	0.841 (0.137)	0.832 (0.151)	0.920 (0.178)	0.902 (0.159)	0.925 (0.161)	0.933 (0.144)
	F1	0.666 (0.064)	0.857 (0.023)	0.771 (0.043)	0.750 (0.043)	0.761 (0.041)	0.751 (0.049)	0.818 (0.043)	0.885 (0.101)	0.722 (0.041)	0.726 (0.018)	0.752 (0.018)	0.708 (0.013)	0.728 (0.132)	0.751 (0.137)	0.890 (0.178)	0.880 (0.159)	0.900 (0.161)	0.913 (0.144)
Avg. Rank	AUC-ROC	11.23	9.70	10.70	7.27	11.50	12.70	13.43	8.27	7.00	7.33	10.20	17.37	6.70	9.83	7.97	8.03	7.40	4.37
	F1	10.30	8.53	9.73	7.00	11.27	12.23	12.30	7.43	6.47	8.00	10.57	16.73	7.53	10.97	8.53	8.90	8.37	6.13
W/T/L (SkewPNN)	AUC-ROC	5/0/10	6/0/9	5/0/10	7/0/8	5/0/10	3/0/12	3/0/12	5/0/10	7/0/8	9/0/6	5/0/10	0/0/15	7/1/7	5/0/10	4/3/8	6/1/8	-	11/1/3
	F1	7/0/8	6/0/9	6/0/9	8/0/7	5/0/10	5/0/10	6/0/9	7/0/8	8/1/6	7/0/8	5/0/10	1/0/14	8/0/7	6/0/9	3/5/7	5/2/8	-	11/1/3
W/T/L (BA-SkewPNN)	AUC-ROC	3/0/12	3/2/10	1/0/14	3/1/11	2/0/13	1/0/14	1/0/14	5/0/10	5/0/10									

their performance is significantly worse than the ‘best-performing’ BA-SkewPNN model.

Alongside the MCB testing procedure, we employ the non-parametric Friedman test to detect statistical differences in model performances [39]. This distribution-free approach evaluates the null hypothesis that the classification performance of all the competing approaches is equivalent based on their average ranks. The test rejects the null hypothesis of statistical equivalence if the computed p-value is less than the specified significance level. We conduct the Friedman test for both imbalanced and balanced classification tasks using the AUC-ROC and F1 metrics at a 5% significance level. For the imbalanced classification tasks, the Friedman test yields p-values of $2.2e^{-16}$ (AUC-ROC) and 0.00001 (F1 metric). For the balanced classification task, the corresponding p-values are 0.0001 (AUC-ROC) and 0.00002 (F1 metric). Since all the calculated p-values are significantly below the threshold of 0.05, we reject the null hypothesis. This indicates that the classification performances of various models differ significantly across both imbalanced and balanced datasets.

Furthermore, to identify which models differ significantly in classifying the imbalanced and balanced datasets, we conduct a post-hoc analysis using the Wilcoxon signed-rank test [76]. This non-parametric statistical procedure conducts pairwise comparisons between individual classifiers, testing the null hypothesis that no significant difference exists between their performances. In our analysis, the Wilcoxon signed-rank test is applied to determine which competing models differ significantly from the proposed SkewPNN and BA-SkewPNN framework at a 5% level of significance. Table 5 summarizes the p-values obtained by comparing the AUC-ROC and F1 metrics of the SkewPNN and BA-SkewPNN models with the competing classifiers for imbalanced and balanced datasets. For the imbalanced classification tasks, the results show that the BA-SkewPNN framework exhibits significant performance differences from all the competing models across both metrics, except for the GHOST model in terms of the F1 metric. Similarly, the SkewPNN model demonstrates significant performance differences from a bunch of competing methods, as determined by both AUC-ROC and F1 metrics. In balanced classification tasks, the p-values indicate that significant performance differences exist between the proposed models and most competing approaches. Overall, the statistical significance tests support the conclusion that the BA-SkewPNN and SkewPNN models exhibit distinct and superior performance compared to other methods for the majority of datasets.

Table 5: Wilcoxon signed-rank test p-values comparing the performance of SkewPNN and BA-SkewPNN with state-of-the-art methods on both imbalanced and balanced datasets. An asterisk (*) indicates significant performance differences between the proposed models and competing methods at the 5% significance level.

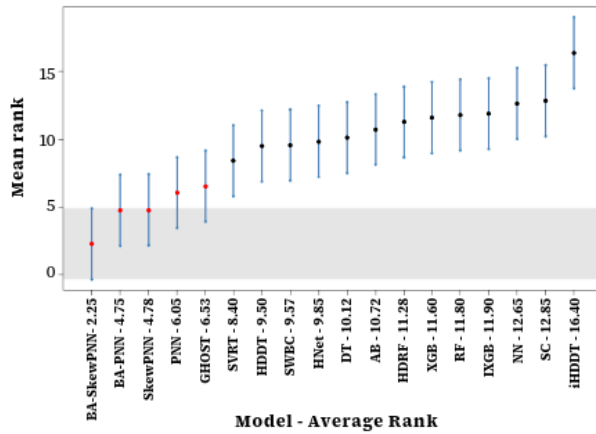
Models	Imbalanced Classification				Balanced Classification			
	SkewPNN vs. Models		BA-SkewPNN vs. Models		SkewPNN vs. Models		BA-SkewPNN vs. Models	
	AUC-ROC	F1	AUC-ROC	F1	AUC-ROC	F1	AUC-ROC	F1
DT	0.0001*	0.0947	0.0001*	0.0060*	0.1817	0.6192	0.0151	0.1384
NN	0.0002*	0.0141*	0.0001*	0.0005*	0.2444	0.2271	0.0252*	0.0442*
AB	0.0001*	0.0606	0.0000*	0.0008*	0.1147	0.3808	0.0002*	0.0660
RF	0.0003*	0.0191*	0.0001*	0.0026*	0.5980	0.7378	0.0483*	0.3193
SC	0.0001*	0.0120*	0.0000*	0.0004*	0.1262	0.3350	0.0021*	0.0416*
SVRT	0.0004*	0.2729	0.0000*	0.0220*	0.0677	0.1514	0.0001*	0.0027*
HDDT	0.0002*	0.0825	0.0001*	0.0148*	0.0416*	0.2622	0.0013*	0.0151*
HDRF	0.0003*	0.0120*	0.0000*	0.0021*	0.2271	0.3882	0.0277*	0.1147
XGB	0.0000*	0.0068*	0.0000*	0.0001*	0.5788	0.7349	0.1514	0.3560
IXGB	0.0004*	0.0448*	0.0001*	0.0024*	0.5980	0.6401	0.0527	0.2216
HNet	0.0023*	0.2283	0.0002*	0.0173*	0.1600	0.4020	0.0042*	0.1006
iHDDT	0.0000*	0.0000*	0.0000*	0.0000*	0.0000*	0.0001*	0.0004*	0.0002*
GHOST	0.0220*	0.7392	0.0001*	0.0836	0.4750	0.7523	0.2807	0.5227
SWBC	0.0002*	0.1841	0.0000*	0.0220*	0.2622	0.3808	0.0075*	0.0319*
PNN	0.0021*	0.0537	0.0003*	0.0003*	0.2778	0.2376	0.0298*	0.0513
BA-PNN	0.8912	0.9723	0.0001*	0.0173*	0.4009	0.5000	0.0008*	0.0101*
SkewPNN			0.0013*	0.0010*			0.0394*	0.0450*
BA-SkewPNN	0.9989	0.9992			0.9657	0.9606		

5. Conclusion and Discussion

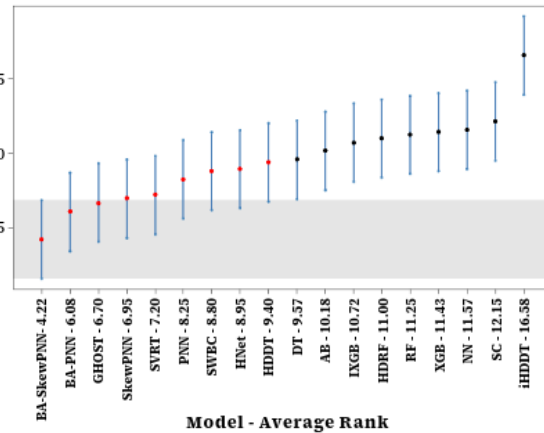
Imbalanced datasets pose complexities in machine learning problems, particularly in classification endeavors. This disparity can prompt models to favor the over-represented class, resulting in compromised

Imbalanced Classification

MCB plot for AUC-ROC

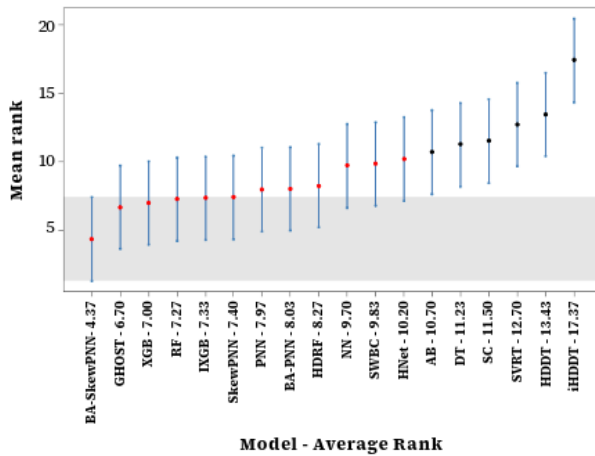


MCB plot for F1



Balanced Classification

MCB plot for AUC-ROC



MCB plot for F1

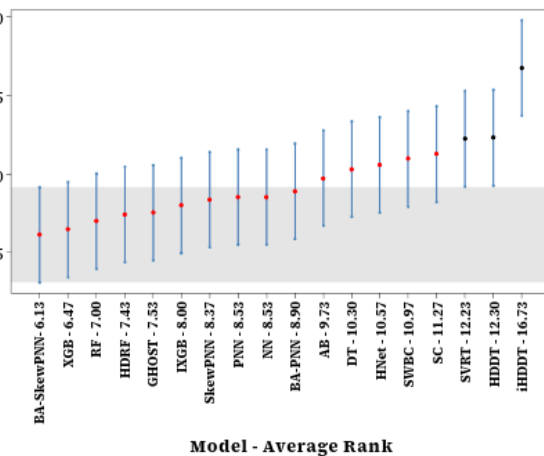


Figure 6: MCB test results for imbalanced and balanced classification tasks were evaluated based on the AUC-ROC and F1 metrics. In the plot, ‘BA-SkewPNN - 2.25’ represents the average rank of the BA-SkewPNN framework (2.25) as computed using the AUC-ROC metric for imbalanced datasets. Similar interpretations apply to other methods.

performance of the minority class. This discrepancy becomes particularly crucial when the minority class holds pivotal insights or embodies infrequent yet pivotal occurrences. In classification scenarios, when class distribution is notably skewed, with one class holding notably more samples (majority class) than others (minority class), the dataset is labeled as imbalanced. This study introduced SkewPNN and BA-SkewPNN algorithms leveraging PNN in tandem with the skew-normal kernel to address the challenge associated with imbalanced datasets. Through this integration, we harness the PNN’s unique capability to provide probabilistic outputs, allowing for a nuanced understanding of prediction confidence and adept handling of uncertainty. Incorporating the skew-normal kernel, renowned for its adaptability in handling non-symmetric data, markedly enhances the representation of underlying class densities. To optimize performance on imbalanced datasets, fine-tuning hyperparameters is crucial, a task we undertake using the Bat optimization algorithm. Our study demonstrates the statistical consistency of density estimates, indicating a smooth convergence to the true distribution with increasing sample size. We have also outlined the theoretical analysis of computational complexity for our proposed algorithms. Furthermore, extensive simulations and real-world data examples comparing various machine learning models affirm the SkewPNN and BA-SkewPNN effectiveness on both balanced and imbalanced data.

SkewPNN can handle data types that are commonly used in classification tasks. Continuous features are inherently well-suited to the skew-normal kernel due to its flexibility in capturing skewness. For categorical features, one-hot encoding is used and SkewPNN is compatible with these transformations. SkewPNN’s ability to capture asymmetrical feature distributions makes it robust for imbalanced data, confirmed by our experimental results and its generalizability across diverse domains. The key limitation of the proposed framework is the scalability issue for large and high-dimensional datasets due to its reliance on storing training instances. This is why our proposal may require more memory for big data problems, and performance may degrade as observed in experimental settings. It may be handled by incorporating a nearest neighbor-based approach, which will determine how many data points from the training set will be considered when calculating distances in the pattern layer of SkewPNN and BA-SkewPNN. A trade-off between the number of nearest neighbors, computational costs, and accuracy will result in a more robust algorithm for big data problems – this can be considered as an immediate future research avenue of this paper. Looking ahead, other future research could also focus on working on imbalanced regression problems [80] where hard boundaries between classes do not exist. We can extend our current work to accommodate regression tasks that involve continuous and even infinite target values (e.g., the age of different people based on their visual appearances in computer vision, where age is a continuous target and can be highly imbalanced).

CRedit authorship contribution statement

Shraddha M. Naik: Data curation; Formal analysis; Investigation; Visualization; Software; Writing - original draft. **Tanujit Chakraborty:** Conceptualization; Methodology; Formal analysis; Investigation; Validation; Writing - original draft; Writing - review & editing. **Madhurima Panja:** Formal analysis; Investigation; Visualization; Writing - review & editing. **Abdenour Hadid:** Supervision; Project administration; Writing - review & editing. **Bibhas Chakraborty:** Supervision; Project administration; Writing - review & editing.

Declaration of competing interest

The authors declare that they have no known competing financial interests or personal relationships that could have appeared to influence the work reported in this paper.

Acknowledgments

We thank the editor, the associate editor, and three reviewers for their insightful comments and constructive feedback.

6. Appendix

Illustrative Example with Numerical values:

We provide an illustrative example with numerical values demonstrating how the SkewPNN algorithm works for imbalanced datasets. For simplicity and easy computation, we consider the training sample of size 10, and Table 6 displays this example dataset with $IR = 4$.

- Class 0 (Majority Class): Clustered around [2,2].
- Class 1 (Minority Class): Clustered around [4,4].
- Our objective is to classify a test point [3.5,3.5].

Table 6: A toy data example with numerical values having ten observations (eight class 0 examples and two class 1 examples).

Feature 1	2.0	2.2	2.4	2.6	2.8	1.8	1.9	2.3	4.0	4.1
Feature 2	2.0	2.2	2.4	2.6	2.8	1.8	2.1	2.1	4.0	4.1
Class	0	0	0	0	0	0	0	0	1	1

Given the input data, the pattern layer computes the similarity between the input vector and the training samples using the Gaussian kernel function (Eqn. 5) in PNN

$$K(x, x_i) = \exp\left(-\frac{d_e^2}{2\sigma^2}\right) \quad (12)$$

and skew-normal kernel function in SkewPNN (with an extra adjusting factor or constant)

$$K(x, x_i) = 2 \exp\left(-\frac{d_e^2}{2\sigma^2}\right) \Phi\left\{\alpha\left(\frac{d_e}{\sigma}\right)\right\}, \quad (13)$$

where d_e is the Euclidean distance between the test point ([3.5,3.5]) and the training points, Φ is the CDF of standard normal distribution, σ and α are the parameters controlling the scale and skewness of the kernels, respectively. It is important to note that for $\alpha = 0$, SkewPNN is simply PNN with a Gaussian kernel. The summation layer aggregates the outputs of the pattern layer neurons for each class. Finally, the output layer provides the probability of the input vector (test sample here) belonging to each class, and the class with the highest probability is chosen as the predicted class. This can be done in two ways: Normalization by dividing the kernel sum for a class by the number of training samples in each class (used in the Algorithm 3.1) or normalizing by dividing the kernel sum for a class by the total sum across all classes. When classes are equal in size, the output of the two normalization methods matches. The normalization by total kernel values produces true posterior probabilities and ensures probabilities sum to 1; therefore, we adopt it for this numerical example for its simplicity (c denotes class label):

$$P(c | x) = \frac{\sum_{i \in c} K(x, x_i)}{\sum_j \sum_{i \in c_j} K(x, x_i)}.$$

We work with this numerical data to provide a detailed calculation for the predicted class using PNN and SkewPNN. The computational results are depicted in Table 7, and we plotted the decision boundaries generated by both the models in Fig. 7.

This illustrative example with numerical values finds that if we use the Gaussian kernel, the majority of class points dominate the probability distribution, leading to the classification of the test point as class 0 (the minority class points have a much smaller contribution). Now, instead of a Gaussian kernel, if we use a skew-normal kernel with the skewness parameter (here we choose $\alpha = -2$), it amplifies the influence of the minority class points, making their probability contribution more significant. This leads to a different

Table 7: Values of different layers of PNN and SkewPNN calculated for the toy example. The networks assign the test input to the class with the highest estimated probability (highlighted in bold).

x_i	$d = x_i - x $	Gaussian Kernel with $\sigma = 1$ (Eqn. 12)	Skew-Normal Kernel with $\sigma = 1, \alpha = -2$ (Eqn. 13)	Class Labels
[2.0, 2.0]	2.1213	0.1053	$2.3283E - 06$	0
[2.2, 2.2]	1.8384	0.1845	$4.3552E - 05$	0
[2.4, 2.4]	1.5556	0.2981	0.0005	0
[2.6, 2.6]	1.2727	0.4448	0.0048	0
[2.8, 2.8]	0.9899	0.6126	0.0292	0
[1.8, 1.8]	2.4041	0.0555	$8.4586E - 08$	0
[1.9, 2.1]	2.1260	0.1043	$2.2102E - 06$	0
[2.3, 2.1]	1.8439	0.1826	$4.1320E - 05$	0
[4.0, 4.0]	0.7071	0.7788	0.1225	1
[4.1, 4.1]	0.8485	0.6976	0.0625	1
Summation layer	sum(kernel values for class 0)	1.9882	0.0347	Predicted class for test point (below)
	sum(kernel values for class 1)	1.4765	0.1850	
Output layer	Prob (class 0 x)	$\frac{1.9882}{(1.9882+1.4765)} = \mathbf{0.5738}$	0.1580	PNN predicts class 0
	Prob (class 1 x)	0.4262	$\frac{0.1850}{(0.0347+0.1850)} = \mathbf{0.8420}$	SkewPNN predicts class 1

classification result, favoring class 1 in this example, as observed in Table 7 and Fig. 7. This example demonstrates how the SkewPNN works for imbalanced binary classification datasets.

Code and Data Availability

To support reproducible research, we are making the code and the data publicly accessible at <https://github.com/7shradha/SkewPNN>.

References

- [1] Abiodun, O.I., Jantan, A., Omolara, A.E., Dada, K.V., Umar, A.M., Linus, O.U., Arshad, H., Kazaure, A.A., Gana, U., Kiru, M.U., 2019. Comprehensive review of artificial neural network applications to pattern recognition. IEEE access 7, 158820–158846.
- [2] Aguilar-Ruiz, J.S., Michalak, M., 2024. Classification performance assessment for imbalanced multiclass data. Scientific Reports 14, 10759.
- [3] Akash, P.S., Kadir, M.E., Ali, A.A., Shoyaib, M., 2019. Inter-node hellinger distance based decision tree., in: IJCAI, pp. 1967–1973.
- [4] Akbani, R., Kwek, S., Japkowicz, N., 2004. Applying support vector machines to imbalanced datasets, in: Machine Learning: ECML 2004: 15th European Conference on Machine Learning, Pisa, Italy, September 20-24, 2004. Proceedings 15, Springer. pp. 39–50.
- [5] Alcal-Fdez, J., Fernandez, A., Luengo, J., Derrac, J., Garcia, S., Sanchez, L., Herrera, F., 2011. Keel data-mining software tool: Data set repository, integration of algorithms and experimental analysis framework. Journal of Multiple-Valued Logic and Soft Computing 17, 255–287.
- [6] Aler, R., Valls, J.M., Boström, H., 2020. Study of hellinger distance as a splitting metric for random forests in balanced and imbalanced classification datasets. Expert Systems with Applications 149, 113264.
- [7] Arnold, B.C., Lin, G.D., 2004. Characterizations of the skew-normal and generalized chi distributions. Sankhyā: The Indian Journal of Statistics 66, 593–606.
- [8] Azzalini, A., 1985. A class of distributions which includes the normal ones. Scandinavian Journal of Statistics 12, 171–178.
- [9] Azzalini, A., 2005. The skew-normal distribution and related multivariate families. Scandinavian journal of statistics 32, 159–188.
- [10] Azzalini, A., 2013. The skew-normal and related families. volume 3. Cambridge University Press.
- [11] Azzalini, A., Capitanio, A., 1999. Statistical applications of the multivariate skew normal distribution. Journal of the Royal Statistical Society: Series B (Statistical Methodology) 61, 579–602.

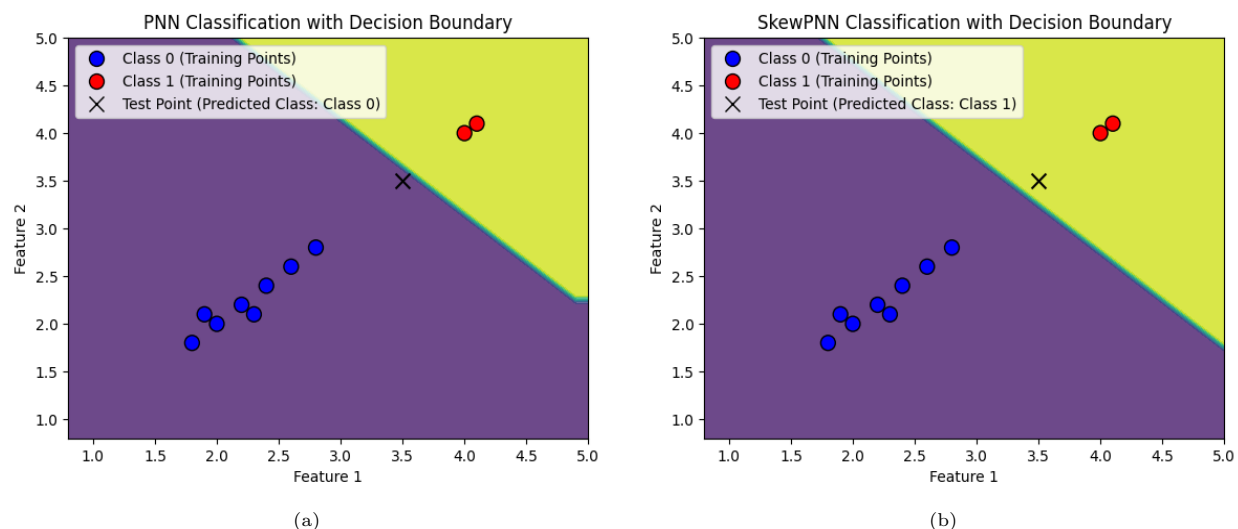


Figure 7: Plots of decision boundaries separating two classes (Class 0 and 1) using (a) PNN algorithm and (b) SkewPNN algorithm. The plot also depicts the predicted class label for the test point.

[12] Azzalini, A., Valle, A.D., 1996. The multivariate skew-normal distribution. *Biometrika* 83, 715–726.

[13] Baesens, B., Höppner, S., Ortner, I., Verdonck, T., 2021. robrose: A robust approach for dealing with imbalanced data in fraud detection. *Statistical Methods & Applications* 30, 841–861.

[14] Barua, S., Islam, M.M., Yao, X., Murase, K., 2012. Mwmote—majority weighted minority oversampling technique for imbalanced data set learning. *IEEE Transactions on knowledge and data engineering* 26, 405–425.

[15] Boonchuay, K., Sinapiromsaran, K., Lursinsap, C., 2017. Decision tree induction based on minority entropy for the class imbalance problem. *Pattern Analysis and Applications* 20, 769–782.

[16] Breiman, L., 2001. Random forests. *Machine learning* 45, 5–32.

[17] Breiman, L., 2017. *Classification and regression trees*. Routledge.

[18] Cano, A., Zafra, A., Ventura, S., 2013. Weighted data gravitation classification for standard and imbalanced data. *IEEE transactions on cybernetics* 43, 1672–1687.

[19] Chaabane, I., Guermazi, R., Hammami, M., 2020. Enhancing techniques for learning decision trees from imbalanced data. *Advances in Data Analysis and Classification* 14, 677–745.

[20] Chakraborty, T., Chakraborty, A.K., 2020a. Hellinger net: A hybrid imbalance learning model to improve software defect prediction. *IEEE Transactions on Reliability* 70, 481–494.

[21] Chakraborty, T., Chakraborty, A.K., 2020b. Superensemble classifier for improving predictions in imbalanced datasets. *Communications in Statistics: Case Studies, Data Analysis and Applications* 6, 123–141.

[22] Chakraborty, T., KS, U.R., Naik, S.M., Panja, M., Manvitha, B., 2024. Ten years of generative adversarial nets (gans): a survey of the state-of-the-art. *Machine Learning: Science and Technology* 5, 011001.

[23] Chawla, N.V., Bowyer, K.W., Hall, L.O., Kegelmeyer, W.P., 2002. Smote: synthetic minority over-sampling technique. *Journal of artificial intelligence research* 16, 321–357.

[24] Chawla, N.V., Lazarevic, A., Hall, L.O., Bowyer, K.W., 2003. Smoteboost: Improving prediction of the minority class in boosting, in: *Knowledge Discovery in Databases: PKDD 2003: 7th European Conference on Principles and Practice of Knowledge Discovery in Databases, Cavtat-Dubrovnik, Croatia, September 22-26, 2003. Proceedings* 7, Springer. pp. 107–119.

[25] Chen, T., Guestrin, C., 2016. Xgboost: A scalable tree boosting system, in: *Proceedings of the 22nd ACM SIGKDD International Conference on Knowledge Discovery and Data Mining*, pp. 785–794.

[26] Cieslak, D.A., Chawla, N.V., 2008. Learning decision trees for unbalanced data, in: *Machine Learning and Knowledge Discovery in Databases: European Conference, ECML PKDD 2008, Antwerp, Belgium, September 15-19, 2008, Proceedings, Part I* 19, Springer. pp. 241–256.

[27] Cieslak, D.A., Hoens, T.R., Chawla, N.V., Kegelmeyer, W.P., 2012. Hellinger distance decision trees are robust and skew-insensitive. *Data Mining and Knowledge Discovery* 24, 136–158.

- [28] Daniels, Z., Metaxas, D., 2017. Addressing imbalance in multi-label classification using structured hellinger forests, in: Proceedings of the AAAI Conference on Artificial Intelligence.
- [29] Das, S., Mullick, S.S., Zelinka, I., 2022. On supervised class-imbalanced learning: An updated perspective and some key challenges. *IEEE Transactions on Artificial Intelligence* 3, 973–993.
- [30] Ding, H., Sun, Y., Huang, N., Shen, Z., Wang, Z., Iftekhar, A., Cui, X., 2023. Rvgan-tl: A generative adversarial networks and transfer learning-based hybrid approach for imbalanced data classification. *Information Sciences* 629, 184–203.
- [31] Dua, D., Graff, C., 2017. Uci machine learning repository. URL: <http://archive.ics.uci.edu/ml>.
- [32] Duda, R.O., Hart, P.E., Stork, D.G., 1995. *Pattern classification and scene analysis*. ed: Wiley Interscience .
- [33] Elor, Y., Averbuch-Elor, H., 2022. To smote, or not to smote? arXiv preprint arXiv:2201.08528 .
- [34] Esposito, C., Landrum, G.A., Schneider, N., Stieff, N., Riniker, S., 2021. Ghost: adjusting the decision threshold to handle imbalanced data in machine learning. *Journal of Chemical Information and Modeling* 61, 2623–2640.
- [35] Farshidvard, A., Hooshmand, F., MirHassani, S., 2023. A novel two-phase clustering-based under-sampling method for imbalanced classification problems. *Expert Systems with Applications* 213, 119003.
- [36] Fernández, A., García, S., Galar, M., Prati, R.C., Krawczyk, B., Herrera, F., 2018a. *Learning from imbalanced data sets*. volume 10. Springer.
- [37] Fernández, A., Garcia, S., Herrera, F., Chawla, N.V., 2018b. Smote for learning from imbalanced data: progress and challenges, marking the 15-year anniversary. *Journal of artificial intelligence research* 61, 863–905.
- [38] Freund, Y., Schapire, R.E., 1995. A desicion-theoretic generalization of on-line learning and an application to boosting, in: *European conference on computational learning theory*, Springer. pp. 23–37.
- [39] Friedman, M., 1937. The use of ranks to avoid the assumption of normality implicit in the analysis of variance. *Journal of the american statistical association* 32, 675–701.
- [40] Genton, M.G., 2005. Discussion of" the skew-normal". *Scandinavian Journal of Statistics* 32, 189–198.
- [41] Ghosh, S., Das, S., 2024. Multi-scale morphology-aided deep medical image segmentation. *Engineering Applications of Artificial Intelligence* 137, 109047.
- [42] Gong, P., Gao, J., Wang, L., 2022. A hybrid evolutionary under-sampling method for handling the class imbalance problem with overlap in credit classification. *Journal of Systems Science and Systems Engineering* 31, 728–752.
- [43] Gu, Q., Tian, J., Li, X., Jiang, S., 2022. A novel random forest integrated model for imbalanced data classification problem. *Knowledge-Based Systems* 250, 109050.
- [44] Gupta, A.K., González-Farías, G., Dominguez-Molina, J.A., 2004a. A multivariate skew normal distribution. *Journal of multivariate analysis* 89, 181–190.
- [45] Gupta, A.K., Nguyen, T.T., Sanqui, J.A.T., 2004b. Characterization of the skew-normal distribution. *Annals of the Institute of Statistical Mathematics* 56, 351–360.
- [46] Han, H., Wang, W.Y., Mao, B.H., 2005. Borderline-smote: a new over-sampling method in imbalanced data sets learning, in: *International conference on intelligent computing*, Springer. pp. 878–887.
- [47] Hanley, J.A., McNeil, B.J., 1982. The meaning and use of the area under a receiver operating characteristic (roc) curve. *Radiology* 143, 29–36.
- [48] He, H., Bai, Y., Garcia, E.A., Li, S., 2008. Adasyn: Adaptive synthetic sampling approach for imbalanced learning, in: *2008 IEEE International Joint Conference on Neural Networks (IEEE world congress on Computational Intelligence)*, IEEE. pp. 1322–1328.
- [49] He, H., Garcia, E.A., 2009. Learning from imbalanced data. *IEEE Transactions on knowledge and data engineering* 21, 1263–1284.
- [50] Koning, A.J., Franses, P.H., Hibon, M., Stekler, H.O., 2005. The m3 competition: Statistical tests of the results. *International journal of forecasting* 21, 397–409.
- [51] Koziarski, M., 2021. Csmote: Combined synthetic oversampling and undersampling technique for imbalanced data classification, in: *2021 International Joint Conference on Neural Networks (IJCNN)*, IEEE. pp. 1–8.
- [52] Krawczyk, B., 2016. Learning from imbalanced data: open challenges and future directions. *Progress in Artificial Intelligence* 5, 221–232.
- [53] Kundu, D., 2014. Geometric skew normal distribution. *Sankhya B* 76, 167–189.
- [54] Lemaitre, G., Nogueira, F., Aridas, C.K., 2017. Imbalanced-learn: A python toolbox to tackle the curse of imbalanced datasets in machine learning. *The Journal of Machine Learning Research* 18, 559–563.
- [55] Li, Y., Jin, J., Tao, H., Xiao, Y., Liang, J., Chen, C.P., 2024a. Complemented subspace-based weighted collaborative representation model for imbalanced learning. *Applied Soft Computing* 153, 111319.

- [56] Li, Y., Wang, S., Jin, J., Tao, H., Nan, J., Wu, H., Chen, C.P., 2024b. Density-based discriminative nonnegative representation model for imbalanced classification. *Neural Processing Letters* 56, 95.
- [57] Li, Y., Wang, S., Jin, J., Zhu, F., Zhao, L., Liang, J., Chen, C.P., 2024c. Imbalanced complemented subspace representation with adaptive weight learning. *Expert Systems with Applications* 249, 123555.
- [58] Mao, K.Z., Tan, K.C., Ser, W., 2000. Probabilistic neural-network structure determination for pattern classification. *IEEE Transactions on neural networks* 11, 1009–1016.
- [59] McDermott, M., Hansen, L.H., Zhang, H., Angelotti, G., Gallifant, J., 2024. A closer look at auroc and auprc under class imbalance, in: *Advances in Neural Information Processing Systems*, pp. 1–39.
- [60] Montana, D., 1992. A weighted probabilistic neural network, in: *Advances in Neural Information Processing Systems*, pp. 1110–1117.
- [61] Naik, S.M., Jagannath, R.P.K., Kuppli, V., 2020. Bat algorithm-based weighted laplacian probabilistic neural network. *Neural Computing and Applications* 32, 1157–1171.
- [62] Parzen, E., 1962. On estimation of a probability density function and mode. *The annals of mathematical statistics* 33, 1065–1076.
- [63] Richard, M.D., Lippmann, R.P., 1991. Neural network classifiers estimate bayesian a posteriori probabilities. *Neural computation* 3, 461–483.
- [64] Ripley, B.D., 1994. Neural networks and related methods for classification. *Journal of the Royal Statistical Society: Series B (Methodological)* 56, 409–437.
- [65] Sağlam, F., Cengiz, M.A., 2022. A novel smote-based resampling technique trough noise detection and the boosting procedure. *Expert Systems with Applications* 200, 117023.
- [66] Sajjadi, M.S., Bachem, O., Lucic, M., Bousquet, O., Gelly, S., 2018. Assessing generative models via precision and recall, in: *Advances in Neural Information Processing Systems*, pp. 1–31.
- [67] Sardari, S., Eftekhari, M., Afsari, F., 2017. Hesitant fuzzy decision tree approach for highly imbalanced data classification. *Applied Soft Computing* 61, 727–741.
- [68] Specht, D.F., 1990a. Probabilistic neural networks. *Neural networks* 3, 109–118.
- [69] Specht, D.F., 1990b. Probabilistic neural networks and the polynomial adaline as complementary techniques for classification. *IEEE Transactions on Neural Networks* 1, 111–121.
- [70] Su, C., Ju, S., Liu, Y., Yu, Z., 2015. Improving random forest and rotation forest for highly imbalanced datasets. *Intelligent Data Analysis* 19, 1409–1432.
- [71] Tahir, M.A., Kittler, J., Yan, F., 2012. Inverse random under sampling for class imbalance problem and its application to multi-label classification. *Pattern Recognition* 45, 3738–3750.
- [72] Thölke, P., Mantilla-Ramos, Y.J., Abdelhedi, H., Maschke, C., Dehgan, A., Harel, Y., Kemtur, A., Berrada, L.M., Sahraoui, M., Young, T., et al., 2023. Class imbalance should not throw you off balance: Choosing the right classifiers and performance metrics for brain decoding with imbalanced data. *NeuroImage* 277.
- [73] Wang, C., Deng, C., Wang, S., 2020. Imbalance-xgboost: leveraging weighted and focal losses for binary label-imbalanced classification with xgboost. *Pattern Recognition Letters* 136, 190–197.
- [74] Wang, Y., Sun, P., 2023. Kernel principle component analysis and random under sampling boost based fault diagnosis method and its application to a pressurized water reactor. *Nuclear Engineering and Design* 406.
- [75] Wei, Z., Zhang, L., Zhao, L., 2023. Minority-prediction-probability-based oversampling technique for imbalanced learning. *Information Sciences* 622, 1273–1295.
- [76] Woolson, R.F., 2007. Wilcoxon signed-rank test. *Wiley Encyclopedia of Clinical Trials* 8, 1–3.
- [77] Xu, B., Wang, W., Yang, R., Han, Q., 2021. An improved unbalanced data classification method based on hybrid sampling approach, in: *2021 IEEE 4th International Conference on Big Data and Artificial Intelligence (BD AI)*, IEEE. pp. 125–129.
- [78] Yang, X., Chen, W., Li, A., Yang, C., Xie, Z., Dong, H., 2019. Ba-pnn-based methods for power transformer fault diagnosis. *Advanced engineering informatics* 39, 178–185.
- [79] Yang, X.S., 2010. A new metaheuristic bat-inspired algorithm, in: *Nature inspired cooperative strategies for optimization (NICSO)*. Springer, pp. 65–74.
- [80] Yang, Y., Zha, K., Chen, Y., Wang, H., Katabi, D., 2021. Delving into deep imbalanced regression, in: *International Conference on Machine Learning, PMLR*. pp. 11842–11851.
- [81] Yen, S.J., Lee, Y.S., 2009. Cluster-based under-sampling approaches for imbalanced data distributions. *Expert Systems with Applications* 36, 5718–5727.

- [82] Yi, J.H., Wang, J., Wang, G.G., 2016. Improved probabilistic neural networks with self-adaptive strategies for transformer fault diagnosis problem. *Advances in Mechanical Engineering* 8, 1–13.
- [83] Yuan, H., Hong, C., Jiang, P.T., Zhao, G., Tran, N.T.A., Xu, X., Yan, Y.Y., Liu, N., 2024. Clinical domain knowledge-derived template improves post hoc ai explanations in pneumothorax classification. *Journal of Biomedical Informatics* 156.
- [84] Yuan, X., Chen, S., Zhou, H., Sun, C., Yuwen, L., 2023. Chsmote: Convex hull-based synthetic minority oversampling technique for alleviating the class imbalance problem. *Information Sciences* 623, 324–341.
- [85] Zhang, G.P., 2000. Neural networks for classification: a survey. *IEEE Transactions on Systems, Man and Cybernetics, Part C (Applications and Reviews)* 30, 451–462.
- [86] Zheng, M., Li, T., Sun, L., Wang, T., Jie, B., Yang, W., Tang, M., Lv, C., 2021. An automatic sampling ratio detection method based on genetic algorithm for imbalanced data classification. *Knowledge-Based Systems* 216, 106800.
- [87] Zhu, Y., Li, C., Dunson, D.B., 2023. Classification trees for imbalanced data: surface-to-volume regularization. *Journal of the American Statistical Association* 118, 1707–1717.